THEORY OF CUTTING WITH LARGE NEGATIVE RAKE CUTTING TOOLS

by

MICHAEL LYNN GOYEN

B.S., Kansas State University, 1975

A MASTER'S THESIS

Submitted in Partial Fulfillment of the

Requirements for the Degree

MASTER OF SCIENCE

Department of Mechanical Engineering

Kansas State University

Manhattan, Kansas

1976

Approved By:

F. C. Appl

Major Professor

TABLE OF CONTENTS

LIST OF TABLES

LIST OF FIGURES

Figure		Page

NOMENCLATURE

a (in.)	Radius of Tool
h (in.)	Depth of Cut
θ (deg.)	Angle of Flat Spot Measured from Vertical
P_1' (lbs./in.)	Normal Force on Equivalent Indenter
P_2' (lbs./in.)	Tangental Force on Equivalent Indenter
b (in.)	Contact Length for Hertz Theory
P_o (lbs./in.^{2})	Maximum Stress on Equivalent Indenter
E (lbs./in.^{2})	Young's Modulus of Elasticity
R (in.)	Radius of Cylinder for Hertz Theory
γ (deg.)	Angle of Inclination of Equivalent Indenter
μ	Coefficient of Friction for Elastic Indenter
μ_2	Coefficient of Friction for Plastic Analysis
η (deg.)	Half the Included Angle of Segment of R_o
S_y (lbs./in.^{2})	Maximum Tensile Stress at Yielding Point
R_e (in.)	Radius of the Equivalent Indenter
R_o (in.)	Undeformed Radius of the Material
θ_e (deg.)	Included Angle of the Segment R_e
ℓ (in.)	Length of Chip Free Surface
λ (deg.)	Angle from Vertical to the Intersection of Tool Radius and Chip Free Surface
ζ (deg.)	Angle of Chip Free Surface

χ	Ratio of the Length of Intersection of R_e and Flat Spot to the Length of Flat Spot
Ω	Ratio of the Length of Intersection of R_o and Flat Spot to the Length of Flat Spot
ψ (rad.)	Angle of Slip-Line
τ (lbs./in.^{2})	Shear Stress
σ (lbs./in.^{2})	Normal Stress
K (lbs./in.^{2})	Yield Point in Shear
P_1 (lbs./in.)	Vertical Component of Cutting Force
P_2 (lbs./in.)	Horizontal Component of Cutting Force
β (deg.)	Included Angle between Chip Free Surface and Equivalent Indenter
P' (lbs./in.)	Normal Force on Cylinder for Hertz Theory
b_e (in.)	Contact Length of Equivalent Indenter
ν	Poisson's Ratio
Λ (rad.)	Angle from Vertical to Point on Tool Surface

CHAPTER I

INTRODUCTION

Since cutting technology is such an essential part of the materials processing needed for the industrialized society of today, there has been a substantial amount of research work done on the subject. By far the greatest amount of work has been done in the areas of metal cutting and metal grinding. The majority of research in metal cutting has been done for the case of orthogonal cutting, which is analyzed as a two-dimensional problem.

The work that has been done on metal cutting shows that it is extremely complex. One of the many difficulties that arise when trying to analyze the problem is that the geometric configuration of the boundaries is not known a priori, as pointed out by Rawaligan and Hazra [1]. And, since the problem involves the elastic-plastic behavior of the workpiece material, the geometry of the boundary is crucial to the solution. In the work done previously it appears that the interaction of the plastic and elastic regions has not been incorporated into the analysis satisfactorily. Furthermore, most work to date has been done considering perfectly sharp, positive rake tools. But in reality the tools cannot be perfectly sharp, and do contain a rounded portion at the tip. This rounded portion also does some of the cutting and to properly understand the process of metal cutting must be included in the analysis. The tool tip is also of extreme importance in relation to tool wear, since to understand the wear that occurs on the flank part of the tool it is necessary to understand the stress distribution and the nature of sliding contact present at the area where the wear occurs.

At present there is increasing interest in cutting with small depths of cut. Many manufactures are interested in using smaller depths while taking wider cuts. This is seen in the new applications of broad nose machining. Also the people involved in grinding research are interested in small depths of cut since this is typical of the cutting action of individual grains during grinding.

In considering cutting problems associated with the rounded tip of the tool, it is believed that it is of major importance at this time to study depths of cut smaller than the nose radius. At these small depths of cut, the tool can be considered as having a large negative rake angle, for which case little research has been done.

CHAPTER II

DESCRIPTION OF THE PROBLEM

Orthogonal cutting with a blunt tool at small depths of cut, is represented schematically in Figs. 1 and 2 by an infinitely long right circular cylinder which has a flat wear spot. The radius is, a, and the angle of the flat spot is, θ, measured from the vertical axis. The depth of cut is h. It is desired to approximate the cutting force components as functions of the tool geometry and the properties of the workpiece material. It is assumed that the cutting velocity is small and temperature effects on workpiece material properties will be neglected. It is further assumed that the workpiece material remains linearly elastic up to the condition of yielding as prescribed by the von Mises criterion. Thus some portions of the workpiece will be in an elastic state and some will be in a plastic state. Interrupted chip formation photographs suggest that the elastic-plastic boundary can be approximated as shown in Fig. 1. Most of the material between the elastic-plastic boundary and the cutting surface of the tool is in the plastic state.

The finite element analysis, which has been applied to an indentation problem by G. Dumes and D. N. Baronet [6], could be used for this problem, but since the cutting problem is unsymmetrical, this would prove to be quite difficult, and require a very large computer. It is therefore desirable to consider simpler approximations to the problem.

THIS BOOK CONTAINS NUMEROUS PAGES WITH DIAGRAMS THAT ARE CROOKED COMPARED TO THE REST OF THE INFORMATION ON THE PAGE.

THIS IS AS RECEIVED FROM CUSTOMER.

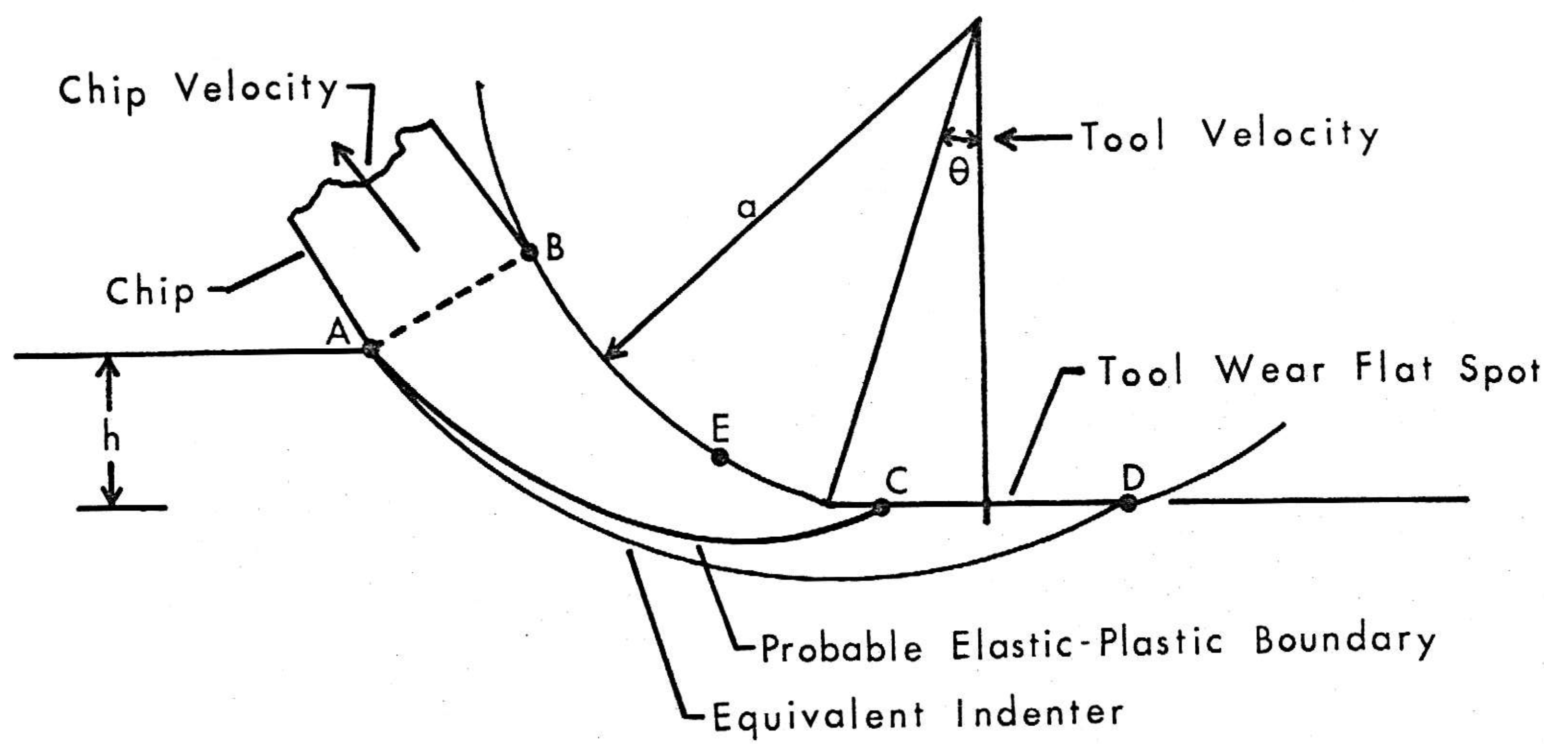

Schematic Of Orthogonal Cutting With A Blunt Tool At Small Depth Of Cut

Figure 1

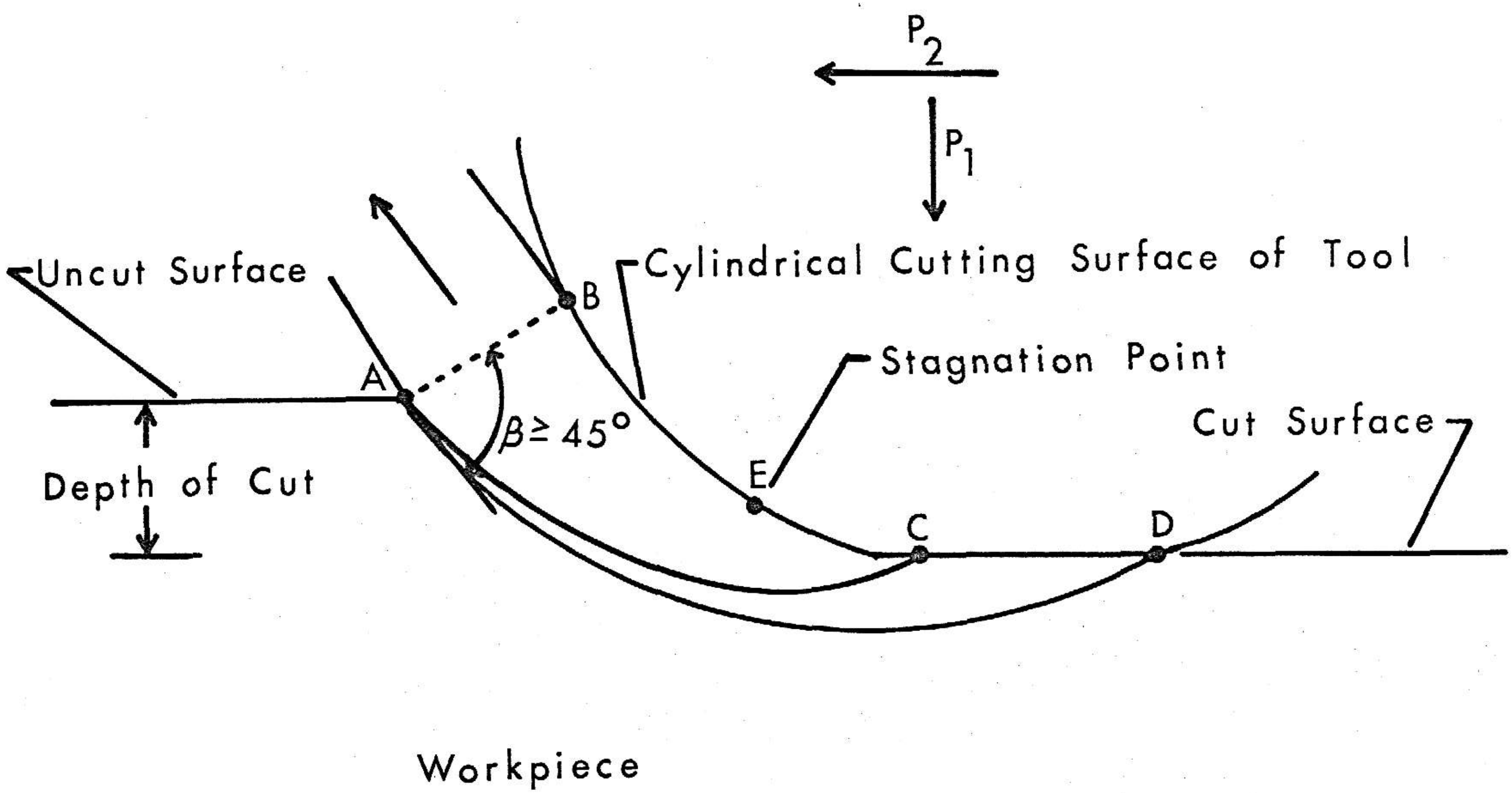

Schematic Of Orthogonal Cutting With A Blunt Tool At Small Depth Of Cut

Figure 2

To determine the cutting forces a method of analysis is needed to properly account for the elastic behavior of the workpiece material outside the elastic-plastic boundary as well as the elastic-plastic behavior of the material within the boundary. This means that the material is at a condition of yield along the boundary and at most points between the boundary and the tool. It is therefore assumed that the material is at a condition of yield along the tool surface from point B to point C, and that it is in an elastic state from point C to point D. It is probable that there will be a chip flow "stagnation point" between point B and point C, such as point E. Above this point it is assumed that the chip is sliding upwards relative to the tool and that it is sliding downwards relative to the tool below point E. The direction of the shear stress due to friction on the tool face will change accordingly.

If the chip were cut away along the line from point A to point B there would be some residual stress distribution. It is believed, however, that the normal and shear stresses along this line are small and can reasonably be neglected. It is, therefore, considered that the surface A-B is equivalent to a traction free surface. It also seems reasonable to assume that slip-lines from the surface of the tool move toward, and eventually intersect, the line A-B.

Since the material is at yield conditions throughout most of the chip forming region between the elastic-plastic boundary and the tool surface, it seems reasonable to assume that the slip-lines will be closely approximated by the usual slip-line theory for ideally plastic materials in which it is assumed that, elastic strains are negligible in comparison to plastic strains. With these assumptions, together with theorems relating to slip-lines published by W. C. Schneider and J. B. Cheatham, Jr. [7], it becomes possible to determine expressions for the normal and shear stress distributions along the tool cutting surface from point B to point C. These results are found in terms of the unknown locations of points A and B. The location of point C is also, as yet, unknown. The vertical and horizontal components of force on the cutting tool due to the surface from B to C can then be found by integrating the stress distributions. These force components are in terms of the locations of points A, B and C.

Although the location of the elastic-plastic boundary is not known, it appears that a cylindrical surface through points A and D which has a tangent at point A, that is 45° or more from line A-B, will lie in the elastic region. The stresses along this surface and throughout the elastic region will be governed by the theory of elasticity. For steady state cutting conditions the horizontal and vertical components of force on this surface will be equal to the corresponding components on the surface of the cutting tool. It seems that a reasonable approximation of the stress distribution along the cylindrical surface is the Hertzian theory for contact of cylindrical surfaces. This theory has been extended to include tangential stress that is proportional to the normal stress. This probably does not represent the actual stress situation, but hopefully by adjusting the shear stress to normal stress ratio, an approximation in the mean can be achieved. Since the normal stress distribution is most important this should be a satisfactory approximation.

In essense these assumptions amount to assuming that an equivalent cylindrical indenter is indenting the elastic material. It is assumed that if the tool were removed the workpiece material along the cylindrical surface would elastically recover to a cylindrical surface of different radius. With these assumptions, the stress distribution on the equivalent indenter can be determined in terms of the location of points A and D, the angle β, and the undeformed radius of the workpiece. These can be integrated to find the vertical and horizontal components of force.

To complete the stress distribution on the tool surface it is assumed that the workpiece is in the elastic state from point C to D and slides on the tool with an assumed coefficient of friction, μ_2. Since this surface is very close to the equivalent indenter in this region, and equivalent normal stress is determined using the stress distribution on the equivalent indenter surface.

Now by adjusting the locations of points A, B and D the vertical and horizontal components of force on the tool and on the equivalent indenter can be made equal. The location of point C is not known but has been assumed to be at the point where the undeformed radius of the workpiece crosses the flat spot surface of the tool. This has been assumed to be just behind the leading edge of the flat spot. This is a rather arbitrary assumption and further consideration of this is needed. At any rate a workable theory of cutting has been established and reasonable results have been obtained for a range of cutting conditions. It appears that more work is needed on the location of points C and D to improve and extend the theory to a wider range of cutting conditions.

CHAPTER III

ELASTIC THEORY FOR THE STRESSES ON THE INDENTER

As previously discussed it was assumed that the tool could be approximated by an equivalent indenter below the elastic-plastic boundary acting in the elastic range. For steady state cutting conditions the horizontal and vertical components of force on this surface will be equal to the corresponding components on the surface of the tool. It seems that a reasonable approximation of the stress distribution along a cylindrical surface is the Hertzian theory for contact of cylindrical surfaces [2]. The original Hertz theory considers only normal contact stresses for this problem and it is desired to include shear stresses as well. This was later done independently by H. Poritsky [3] and by J. O. Smith and Chang Keng Lin [4].

The equivalent indenter is described by the radius R_e, and must pass thru points A and D as shown in Fig. 4. The radius of the workpiece is R_o, and is assumed to be the radius the material would elastically rebound to if the load of the equivalent indenter was removed.

From the Hertz theory

$$P' = \tfrac{1}{4}\, b\, P_o \tag{1}$$

$$b = \frac{4P_o \left(\frac{1 - \nu_1^2}{E_1} + \frac{1 - \nu_2^2}{E_2} \right)}{\left(\frac{1}{R_1} + \frac{1}{R_2} \right)} \tag{2}$$

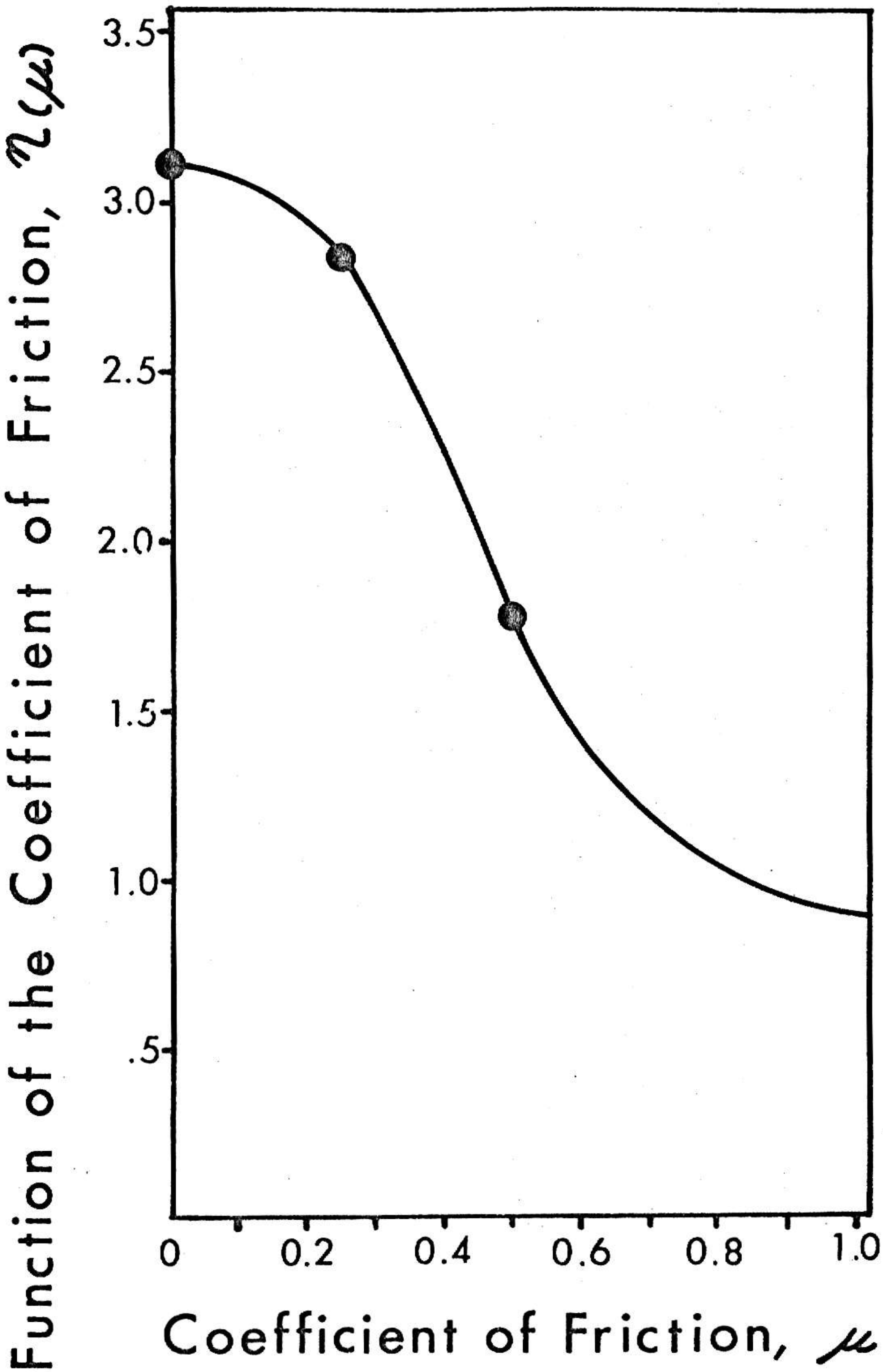

Graph Of The Function $\eta(\mu)$

Figure 3

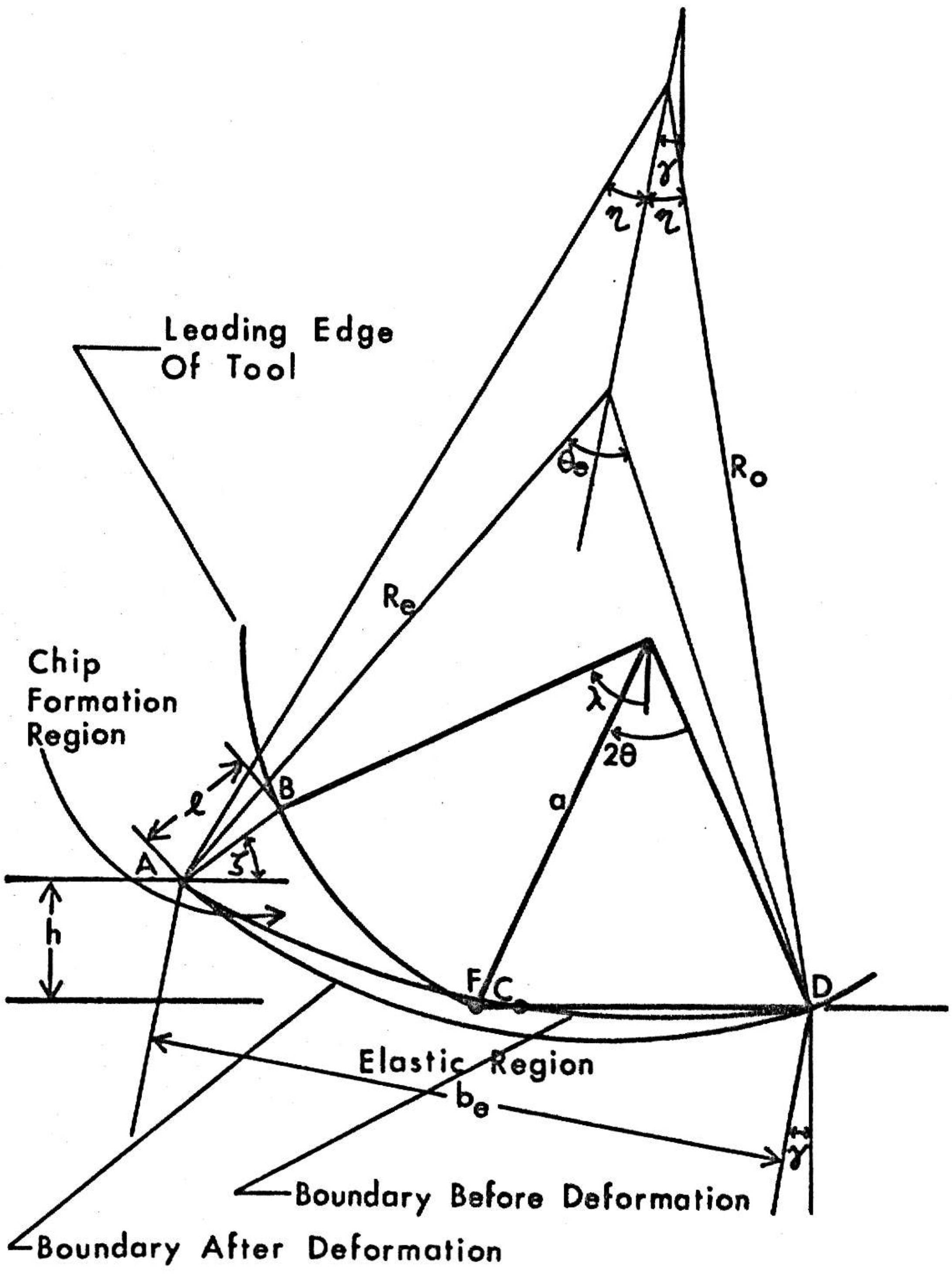

Geometry Of The Equivalent Indenter

Figure 4

Where P' is the load per unit length in the normal direction, b is the width of contact, P_o is the maximum normal stress, ν is Poisson's ratio, E is Young's modulus of elasticity, and R is the radius of curvature. The subscripts 1 and 2 refer to the tool and material respectfully.

Now of interest is the initial point of yielding. Work done by G. M. Hamilton and C. E. Goodman [5], who used the work of Poritsky [3], shows that the first yielding occurs when the maximum normal stress becomes

$$P_o = \left(\frac{S_y}{\sqrt{3}}\right) \eta(\mu) \qquad (3)$$

where $\eta(\mu)$ is a function of the coefficient of friction, μ. From their data the relationship for $\eta(\mu)$ was plotted and is shown in Fig. 3.

In applying the work of Hertz, Poritsky, and Goodman it is first assumed that the tool is rigid, making $E_1 = \infty$. The radius of the equivalent indenter is R_e and the undeformed radius of the workpiece is R_o, which, according to the Hertz theory, is negative since it is a cylindrical seat. The length of contact of the equivalent indenter is b_e and the angle of inclination of the indenter is γ, as seen in Fig. 4.

By making these assumptions equation (1) becomes

$$P_1' = \tfrac{\pi}{4}\, b_e\, P_o \qquad (4)$$

where P_1' is the normal unit load on the indenter. From equation (2) we now get

$$R_e = \frac{b_e E_2}{4P_o (1 - \nu_2^2)} + R_o \tag{5}$$

P_o is still defined by its relationship with the function, $\eta(\mu)$, by

$$P_o = \left(\frac{S_y}{\sqrt{3}}\right) \eta(\mu) \tag{6}$$

The force on the tool in the tangential direction, P_2', can be described by

$$P_2' = \mu P_1' \tag{7}$$

since the shear stress is proportional to the normal stress.

From the geometry of the equivalent indenter in Fig. 4, θ_e, which is the central angle of the segment of the equivalent indenter is found to be

$$\theta_e = 2 \sin^{-1} \left(\frac{b_e}{2R_e}\right). \tag{8}$$

Also, from this geometry, the depth of cut, h, is

$$h = b_e \sin(\gamma) \tag{9}$$

and the contact length, b_e, is

$$b_e = 2R_e \sin\left(\frac{\theta_e}{2}\right) \tag{10}$$

Another equation to define the angle of indenter inclination, γ, is found from the geometry in Fig. 4 and equations (11) and (12) can be written by summing vertical and horizontal distances

$$\ell \cos(\zeta) + a \sin(\lambda) + a \sin(\theta) = b_e \cos(\gamma) \tag{11}$$

$$\ell \sin(\zeta) + a \cos(\lambda) + h = a \cos(\theta) \tag{12}$$

By combining equations (11) and (12) we get

$$\tan(\zeta) = \frac{a \cos(\theta) - a \cos(\lambda) - h}{b_e \cos(\gamma) - a \sin(\lambda) - a \sin(\theta)} \tag{13}$$

From equation (9) the expression for b_e is

$$b_e = \frac{h}{\sin(\gamma)} \tag{14}$$

by the substitution of equation (14) into equation (13) we get

$$\tan(\gamma) = \frac{(h/a)\ \tan(\zeta)}{\cos(\theta) - \cos(\lambda) - (h/a) + \tan(\zeta)\ [\sin(\lambda) + \sin(\theta)]} \tag{15}$$

Since these equations must be satisfied simultaneously it was necessary to have more constraints to define the solution. To do this it was decided to put some restrictions on the radius of curvature, R_o and R_e. We chose to limit the intersection of R_e and a horizontal line drawn from the flat spot to be to the left of point F, shown in Fig. 4. From a practical standpoint this means that the equivalent indenter cannot intersect the cutting tool surface. This was done by using the ratio, χ, defined by

$$\chi = \frac{2R_e\ \sin(\theta_e/2 - \gamma)}{2\ a\ \sin\ (\theta)} \tag{16}$$

or

$$\chi = \frac{R_e\ \sin(\theta_e/2 - \gamma)}{a\ \sin\ (\theta)} \tag{17}$$

To satisfy the requirement specified above, the ratio, χ, must be greater than or equal to 1.0.

$$\chi \geq 1.0 \tag{18}$$

Similarly, a ratio, Ω, was defined by

$$\Omega = \frac{2R_o \sin(\eta - \gamma)}{2\ a \sin(\theta)} \tag{19}$$

or

$$\Omega = \frac{R_o \sin(\eta - \gamma)}{a \sin(\theta)} \tag{20}$$

By setting

$$\Omega \leq 1.0 \tag{21}$$

the intersection of R_o and the flat spot is forced to be to the right of point F, which is the point C, shown in Fig. 4.

By using a computer and an iteration technique, the previous equations can be solved simultaneously to obtain the normal load, P_1', and tangental load, P_2', that are present on the equivalent indenter.

These components of force were then used to determine the equivalent vertical and horizontal components of force, P_1 and P_2.

$$P_1 = P_1' \cos(\gamma) - P_2' \sin(\gamma) \tag{22}$$

$$P_2 = P_1' \sin(\gamma) + P_2' \cos(\gamma) \tag{23}$$

Thus we can find the vertical and horizontal loads that would be necessary for an equivalent indenter of radius, R_e, to cause the prescribed deformation in a material having the radius R_o. These should be equal to the corresponding loads acting on the surface of the tool.

CHAPTER IV

WORK BY SCHNEIDER AND CHEATHAM

W. C. Schneider and J. B. Cheatham, Jr. did some work on indentation analysis for general shapes of surface boundaries and punch profiles [7]. They present an analysis that frees the designer from the need to assume a slip-line field when calculating the pressure beneath a punch. Theorem I, of their presentation, reveals that the pressure is independent of the slip-line shape and depends only on its terminal points. They also point out that for many practical problems, information about the terminal points is known, even though the slip-line shape is unknown.

So, according to this theorem, the indentation pressure at any point on the punch depends only on the angle between the tangent to the punch surface and the boundary at the two ends of a slip-line through the point in question. The general problem is shown in Fig. 5.

They applied Theorem I to this general problem, and arrived at equation (24) for the normal pressure present at point G on the punch.

$$P_G = \sigma_H + K \sin(2\psi_H) + K \sin(2\psi_G) + 2K(\psi_H - \theta_H + \psi_G - \theta_G) \qquad (24)$$

The corresponding shear stress is found to be

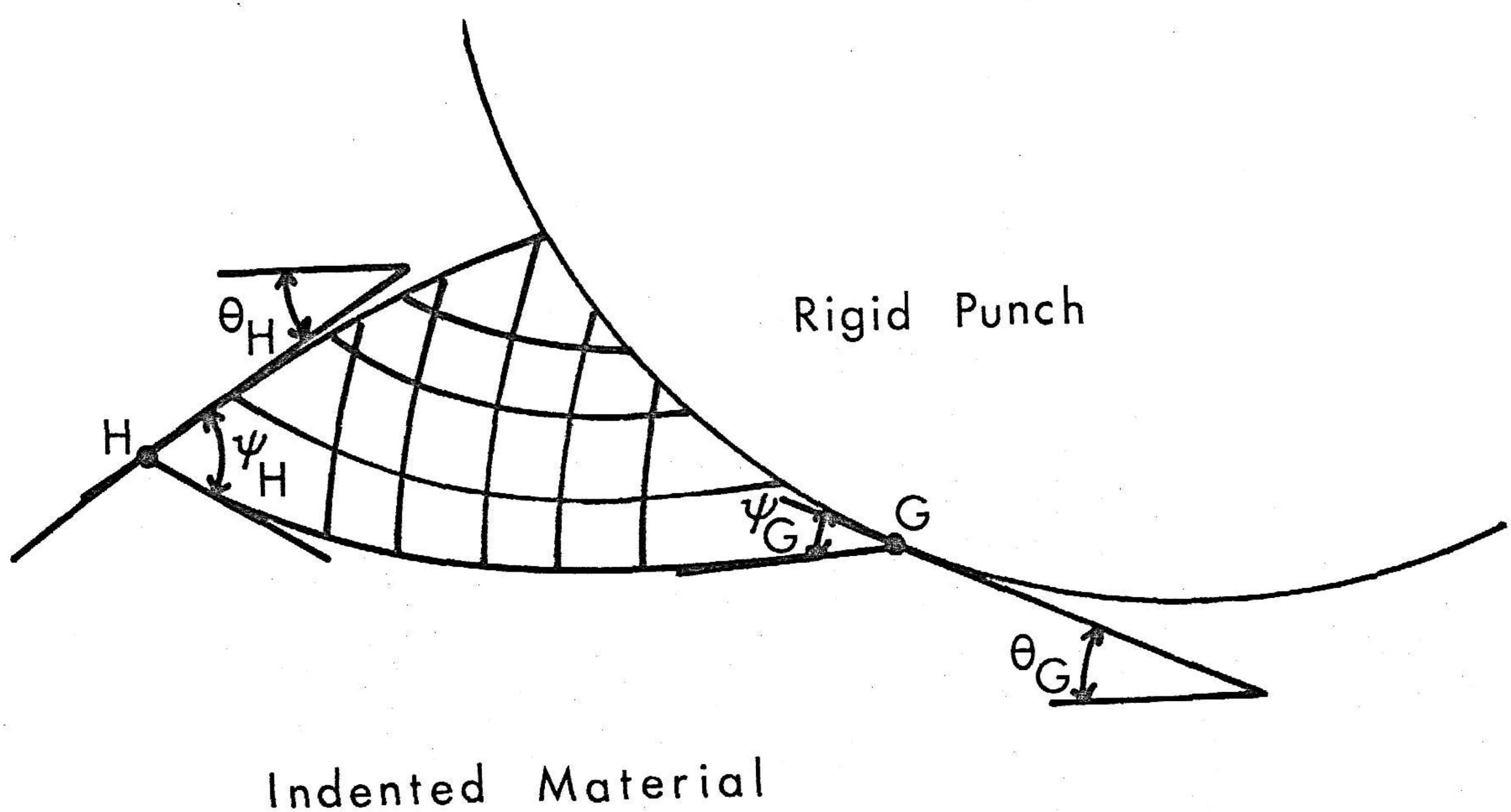

Geometry Of Punch Slip-Lines

Figure 5

$$\tau_G = -K \cos (2\psi_G). \tag{25}$$

It is also noted that for a perfectly lubricated punch $\tau_G = 0$.

Schneider and Cheatham applied this theory to the case of a frictionless punch with zero shear and normal stress on the remaining boundary. Making these assumptions and applying the Tresca or von Mises yield condition they found $\psi_G = \psi_H = \pi/4$ radians or 45°.

For a stress-free boundary, $\sigma_H = 0$, and hence the pressure at point G can be written as

$$P_G = 2K(\frac{\pi}{2} + 1.0 - \theta_H - \theta_G) \tag{26}$$

But even this case is not easily solved since for irregular boundaries the angle θ_H is not known without knowing the shape of the slip-line. So, to be easier and more practical, the problem of a smooth punch and straight, stress-free boundaries was studied. For this case they assumed a horizontal stress-free boundary which gave them $\sigma_H = 0$ as well as $\theta_H = 0$ and $\psi_H = \pi/4$. ψ_G is also equal to $\pi/4$ since the punch is assumed smooth and frictionless. From these assumptions the normal pressure at G becomes

$$P_G = K \sin(2 \frac{\pi}{4}) + K \sin(2 \frac{\pi}{4}) + 2K(\frac{\pi}{4} - 0 + \frac{\pi}{4} - \theta_G) \tag{27}$$

or

$$P_G = 2K(1 + \frac{\pi}{2} - \theta_G). \tag{28}$$

This now becomes a very easy and useful solution since most punch problems have straight stress-free boundaries and this analysis is easy to apply without prior knowledge of the slip-line field.

CHAPTER V

PLASTIC THEORY FOR THE STRESSES ON THE TOOL

To analyze the stresses on the tool face it can be seen that most of the material in front of the leading edge is undergoing plastic deformation. Therefore it is assumed that slip-line field theory is applicable in this region. Since the slip-line field is not known and cannot easily be found, it is necessary to make some assumptions. It is believed that normal and shear stresses are small along line A-B in Fig. 1 and can be neglected, so the surface containing line A-B is assumed to be stress free. This surface is defined by the angle ζ in Fig. 4. The region undergoing plastic deformation was assumed to be from point B to the intersection of the tool flat wear spot and the undeformed radius of the workpiece material below the equivalent indenter, point C in Fig. 4. It is believed that along the leading edge of the tool the workpiece material is undergoing plastic deformation from point B to point C as seen in Fig. 1. In the region behind point C it is considered that sliding elastic conditions prevail.

To analyze the stresses present on the leading edge of the tool governed by plastic conditions, the work done by W. C. Schneider and J. B. Cheatham, Jr. [7], on the indentation of plastic material with general punch profiles was used. As they showed the normal stress present at point G, on the tool is

$$P_G = \sigma_H + K\sin(2\psi_G) + K\sin(2\psi_H) + 2K(\psi_H - \zeta + \psi_G - \Lambda) \quad (29)$$

and the shear stress at point G is

$$\tau_G = K\cos 2\psi_G \quad (30)$$

where ψ_H is the slip-line angle at point H on the chip free surface and ψ_G is the slip-line angle at point G on the tool as shown in Fig. 6. σ_H is the normal stress at point H, ζ is the angle from the horizontal of the tangent to the surface at point H, and Λ is the angle from the horizontal of the tangent to the surface at point G. The constant K is defined as the yield point in shear. Since it has been assumed that the surface A-B is stress free this means that $\sigma_H = 0$, and by assuming that the Tresca or von Mises yield condition applies $\psi_H = \pi/4$ radians or 45 degrees [7]. Using these assumptions the stresses can now be written as

$$P_G = K\sin(2\psi_G) + K\sin(\frac{2\pi}{4}) + 2K(\frac{\pi}{4} - \zeta + \psi_G - \Lambda) \quad (31)$$

and

$$\tau_G = K\cos(2\psi_G). \quad (32)$$

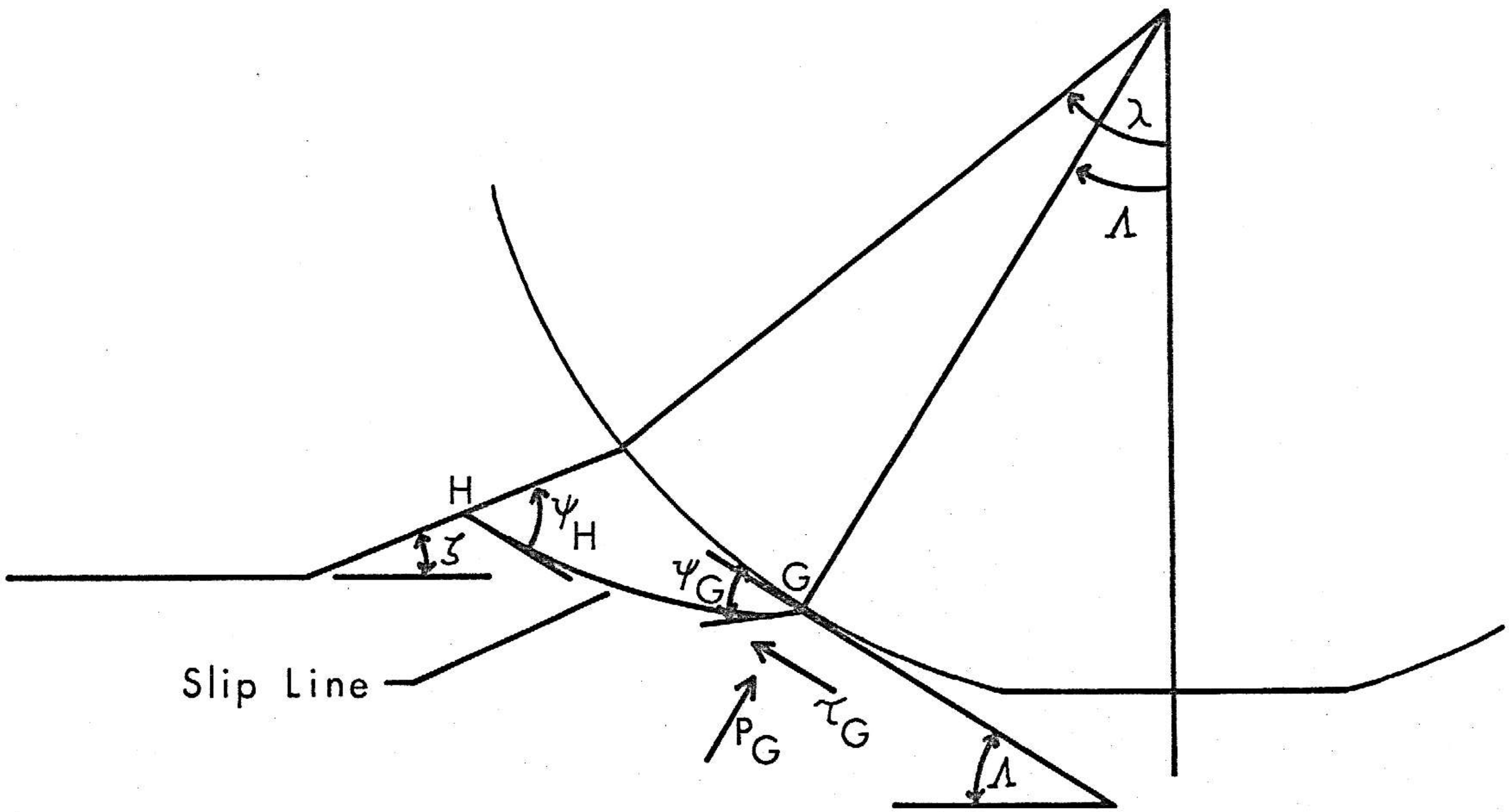

Geometry Of The Slip-Lines For The Cutting Tool

Figure 6

These equations apply from the point of intersection of the chip free surface and the tool, point B, down the leading edge of the tool to the point of intersection of the undeformed radius, R_o, and the flat spot, point C.

To determine the angle, ψ_G, of the slip-line at point G an approximate relation between shear stress and normal stress was used

$$\tau = K(1 - e^{-\mu_2(\sigma/K)}) \tag{33}$$

along with equation (32) for each point in the plastic range. The relationship presented in equation (33) was assumed because the relationship between shear stress and normal stress with low normal pressures at a sliding interface is

$$\tau = \mu_2 \sigma \tag{34}$$

in the direction opposing the motion and that at yield conditions

$$\tau_{max} = K, \tag{35}$$

by the definition of K. Having these conditions an exponential curve was used to approximate the transitional relationship. The general equation for an exponential curve with an upper limit of K is

$$\tau = K(1 - e^{-\alpha(\sigma/K)}) \tag{36}$$

and the slope at $\sigma = 0$ is found to be

$$\left.\frac{d\tau}{d\sigma}\right|_{\sigma = 0} = K(\alpha) \frac{1}{K} e^{-\alpha(\sigma/K)}\Big|_{\sigma = 0} = \alpha \tag{37}$$

which for this problem is equal to the coefficient of friction, μ_2. From this, the expression for the shearing stress is

$$\tau = K(1 - e^{-\mu_2(\sigma/K)}) \tag{38}$$

as shown in Fig. 7.

Knowing the normal stresses and the shear stresses at every point on the nose of the tool it is possible to integrate these stresses to obtain the resultant forces in the horizontal and vertical directions.

In the case of small flat spots there can be a point where the material can't be pushed ahead by the tool, so it slips under the tool surface; this creates a stagnation point. This is caused by the increasingly large negative rake that is found further down the tool edge. A similar critical rake angle was discussed in the work of C. Rubenstein, F. K. Groszmen, and F. Koenigsberger [8], who cut lead with large negative rake tools. Their work showed the critical rake angle to be in the range of (65 to 75° negative rake). These values

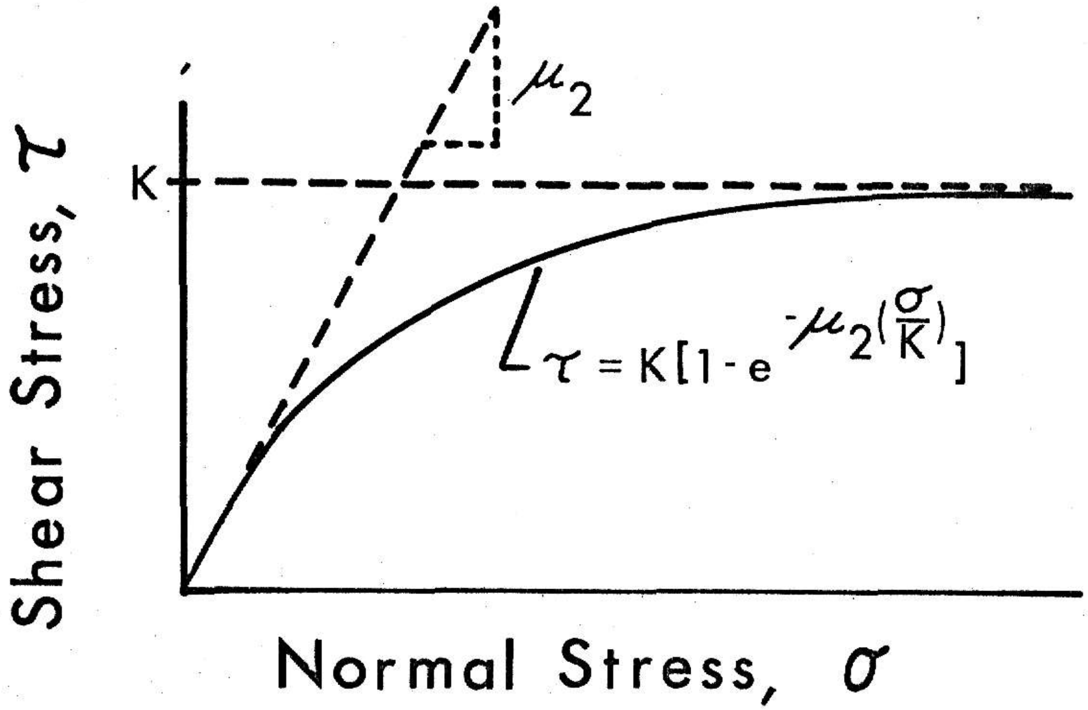

Shear And Normal Stress Relationship On The Surface Of The Tool

Figure 7

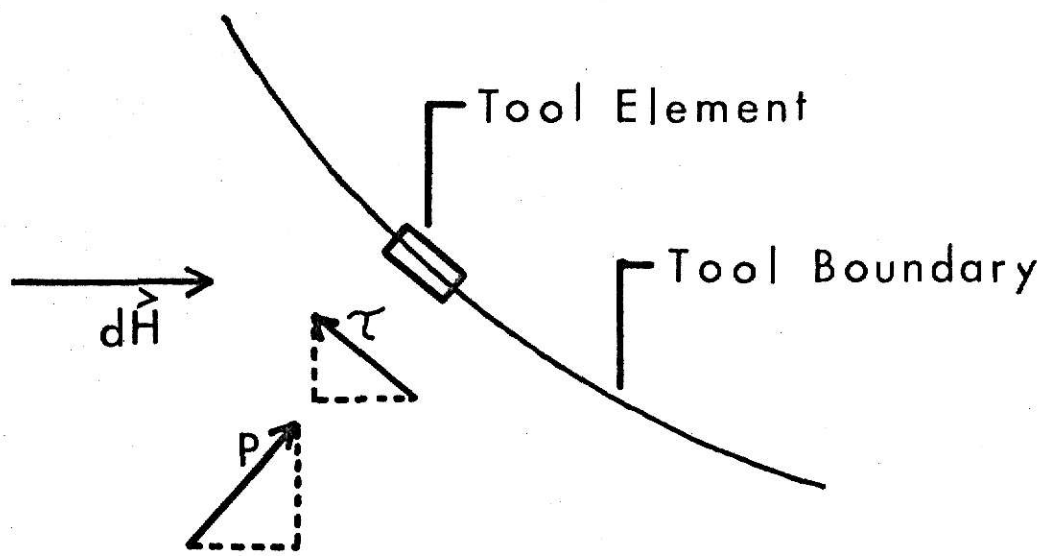

Stresses On The Surface Of The Tool

Figure 8

do not apply directly to a tool with rounded nose since they used tools with straight rake faces.

To decide where this stagnation point occurred for a tool with rounded nose an element with a normal stress, P, and a shearing stress, τ, acting on it, as shown in Fig. 8, was studied. The horizontal component of force on the element, $d\vec{H}$, was considered. If $d\vec{H}$ is positive there is positive work being done by the tool, but if $d\vec{H}$ is negative then that increment of the tool is performing negative work. Since the idea of doing negative work doesn't seem reasonable, it was assumed that the point on the tool when $d\vec{H} = 0$ is the point where the direction of the material sliding reverses its direction, and hence the direction of the shear stress, τ, changes its direction to oppose the reversed motion of the material as seen in Fig. 9. Using this guideline will keep $d\vec{H}$ positive and insure that all increments of the tool nose do positive work. It should be noted, that although the workpiece material at the tool interface may be moving downward relative to the tool, it is still moving upward relative to the workpiece, thus the slip-lines can still move to the chip free surface.

It was previously assumed that all points between points C and D, in Fig. 4, were to be considered in an elastic state. Since this surface is very close to the equivalent indenter in this region, an equivalent normal stress is determined using the stress distribution on the equivalent indenter surface. To perform this transformation it was necessary to adjust the stresses for the angle of indenter inclination,

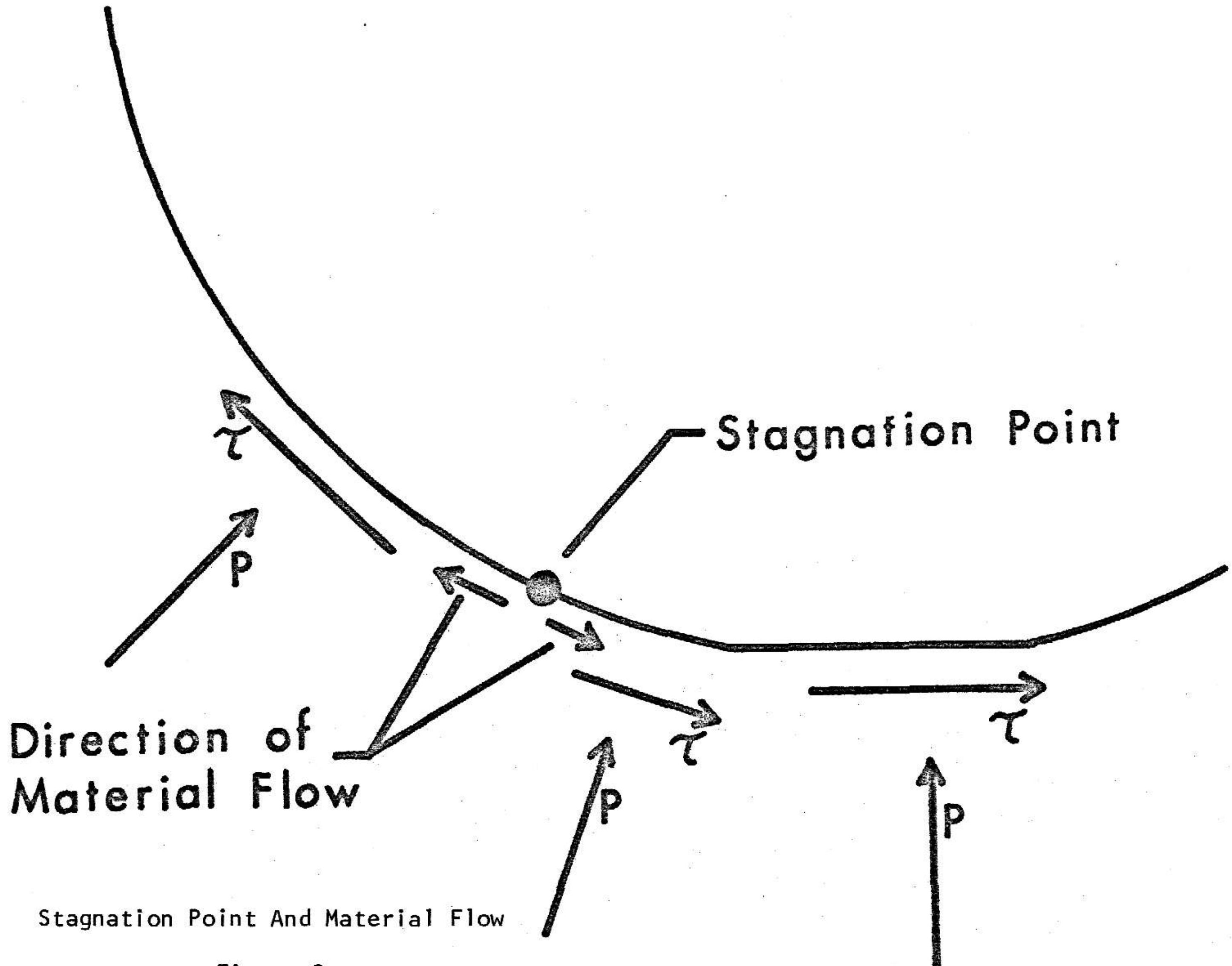

Stagnation Point And Material Flow

Figure 9

γ. An element inclined by the angle γ, with a normal stress, S_1, and a shear stress, τ_1, is shown in Fig. 10. From this element a partial element is drawn, as shown in Fig. 11. Applying statics to the partial element in Fig. 11, gives an expression for σ as

$$\sigma = S_1 \cos^2(\gamma) - \mu S_1 \cos(\gamma) \sin(\gamma) + S_2 \sin^2(\gamma) - \mu_1 S_1 \sin(\gamma) \cos(\gamma) \quad (39)$$

Since the angle, γ, is small the term $\sin^2(\gamma)$ can be neglected; making the expression for σ equal to

$$\sigma = S_1 \cos^2(\gamma) - S_1\mu \cos(\gamma) \sin(\gamma) - \mu_1 S_1 \sin(\gamma) \cos(\gamma) \quad (40)$$

The expression for the shearing stress, τ, on this surface is assumed to be

$$\tau = \mu_2 \sigma \quad (41)$$

since it was assumed that the material in this area is in the elastic range and the shear stress is then proportional to the normal stress.

Now by integrating the vertical and horizontal components of the stresses over the tool surface the vertical and horizontal components of cutting force are obtained.

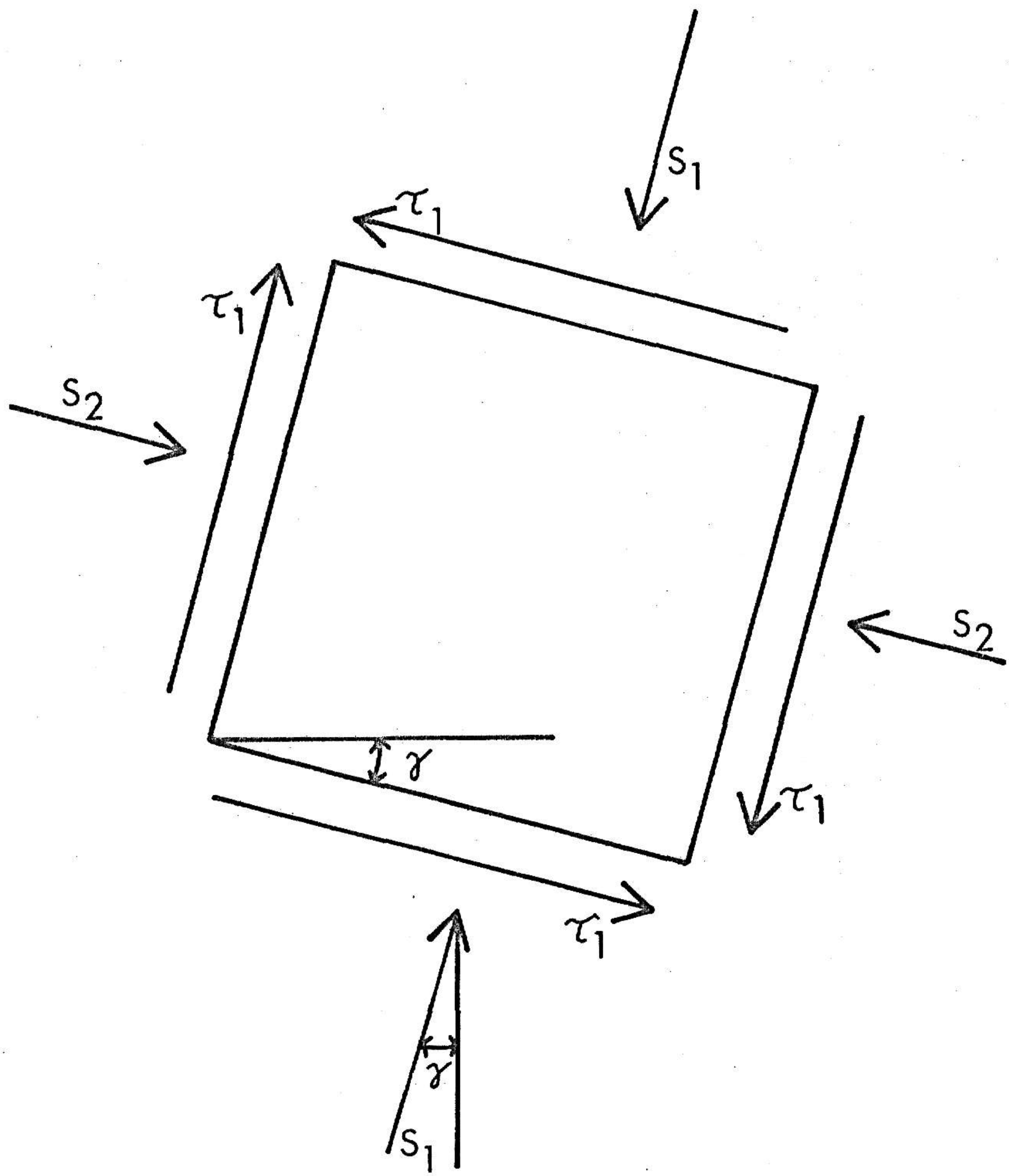

Element Stresses For The Elastic Boundary

Figure 10

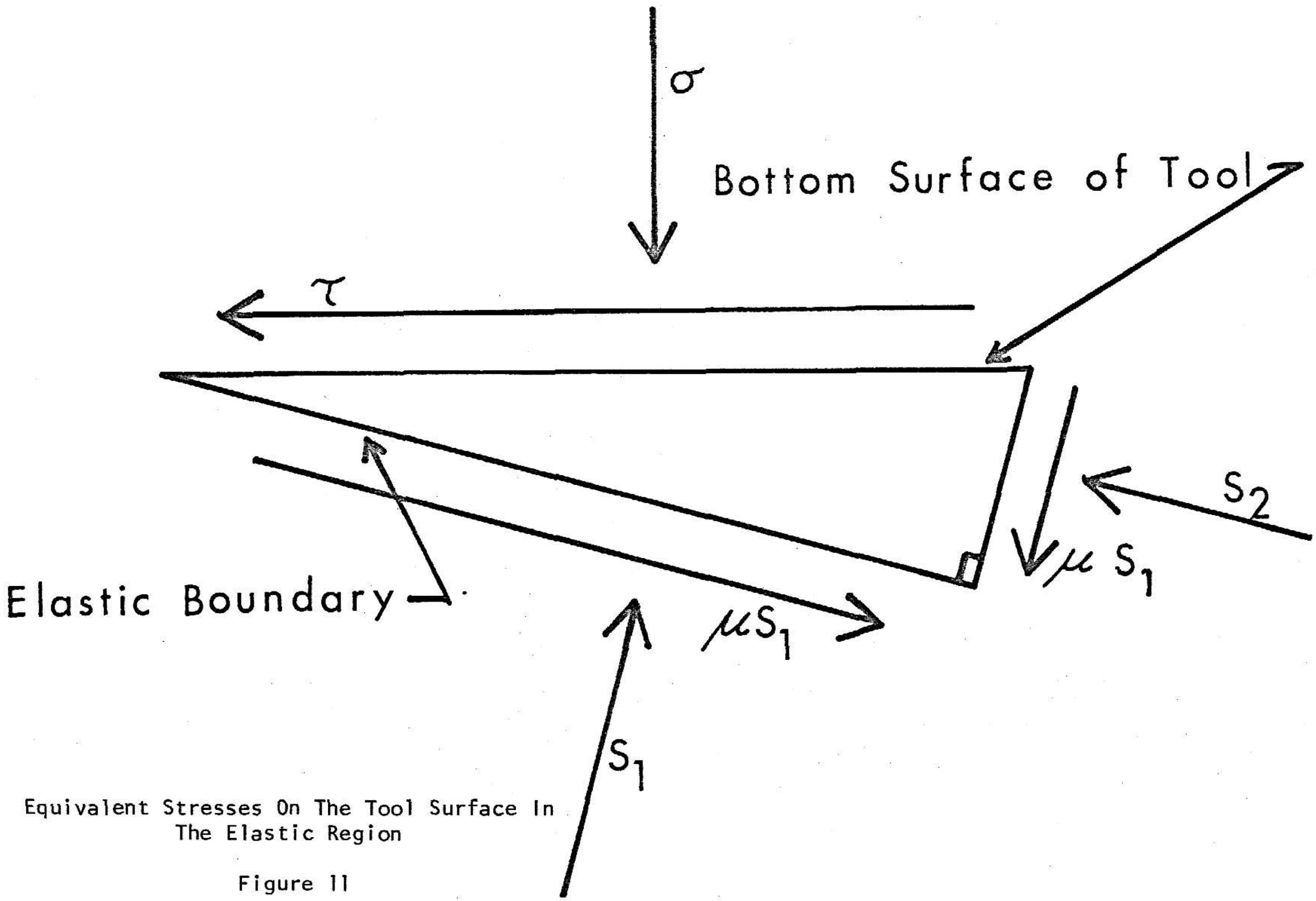

Equivalent Stresses On The Tool Surface In
The Elastic Region

Figure 11

CHAPTER VI

PROCEDURE TO OBTAIN THE COMBINED ELASTIC-PLASTIC SOLUTION

The two previously described parts of the solution both contain variables which are to be determined by matching the elastic and plastic solutions. The major variable that is unknown is the angle of the chip free surface, ζ. By changing ζ it was possible to match the vertical components of force. The horizontal components of force were then matched by changing the coefficient of friction acting on the equivalent indentor, μ. By adjusting μ in this manner it is hoped that the shear stress distribution on the equivalent indenter is approximated in the mean.

This procedure was programmed for the computer and proved to be workable for part of the range of the cutting variables.

CHAPTER VII

RESULTS

To determine if the theory represents a satisfactory approximation to the cutting problem it is necessary to compare it with experimental results. A literature search revealed that there has been little research done for small depths of cut with negative rake tools. The best experimental results were obtained by M. Es. Abdelmonein and R. F. Scrutton [9].

In comparing theoretical and experimental results, it is necessary to duplicate the problem as much as possible. Abdelmonein and Scrutton did tests using brass, aluminum, and zinc, as the cutting material. The results obtained with free cutting brass were used for comparison due to the ease in which the material properties could be found. Material properties for aluminum and zinc vary considerably and hence, it is difficult to establish the values which correspond to their tests. The free cutting brass plates used by Abdelmonein and Scrutton were 62 percent Cu, 35 percent Zn, and 3.25 percent Pd, and were stress relieved at 475° F for one hour prior to cutting. The tensile yield strength, S_y, is found to be 58,000 psi for a brass plate of that composition and stress relieved under those conditions. The radius of the tool, a, is 0.003 inches to match the tool radius used by Abdelmonein and Scrutton.

The value of the coefficient of friction on the surface of the cutting tool, μ_2, was taken to be 0.7. The coefficient of friction can vary over a considerable range and depends largely on the surface conditions. Since the surface is clean due to the fact that it is a freshly cut surface the coefficient of friction is probably higher than might be expected. Further study of friction in the cutting region is needed to more accurately establish μ_2.

The computer program, shown in Appendix I, contains a number of iteration loops to match the previously explained equations simultaneously. Due to the nature of the problem and the assumptions made the computer program is not capable of obtaining a solution for every problem, but can only find the solutions to problems in certain ranges. With further refinement it should be possible to expand this analysis to a larger range of cutting conditions.

Numerical results obtained using the present analysis are plotted in Figs. 12 and 13. By the nature of the program it was not possible to find a solution with the flat wear spot angle, θ, equal to 0. For this case it was necessary to plot the cutting forces versus the flat spot wear angle and extrapolate to a zero flat spot. This was done to aid in the comparison with the experimental data, since the cutting tool used by Abdelmonein and Scrutton did not have a flat spot. Since the values corresponding to $\theta = 0$ are found by the extrapolation of the curves the corresponding points in Figs. 14 and 15 are approximations based on the intersection of the curves and the vertical axis, $\theta = 0$, in Figs. 12 and 13.

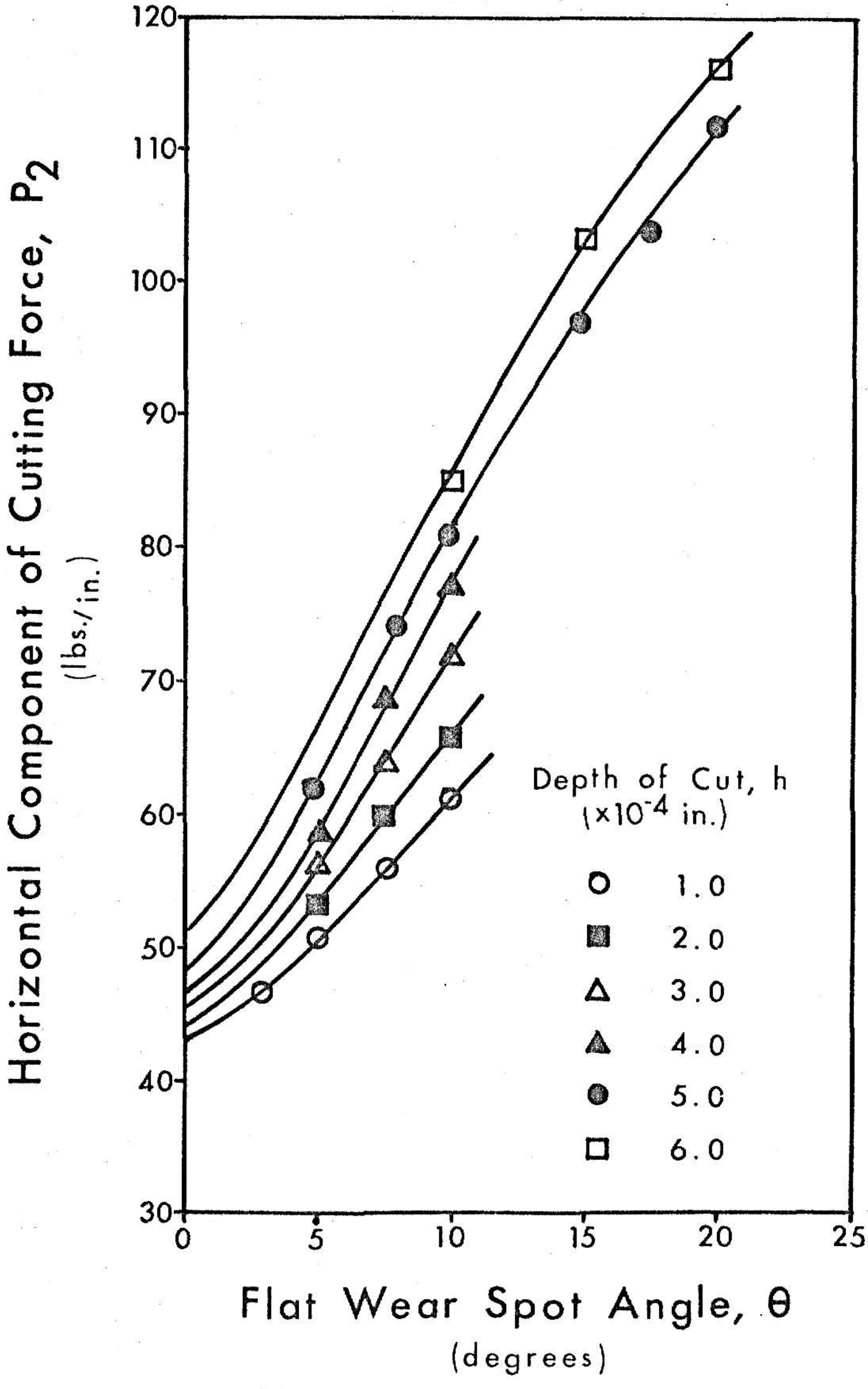

Horizontal Component Of Cutting Force, P_2 versus Wear Spot Angle, θ

Figure 12

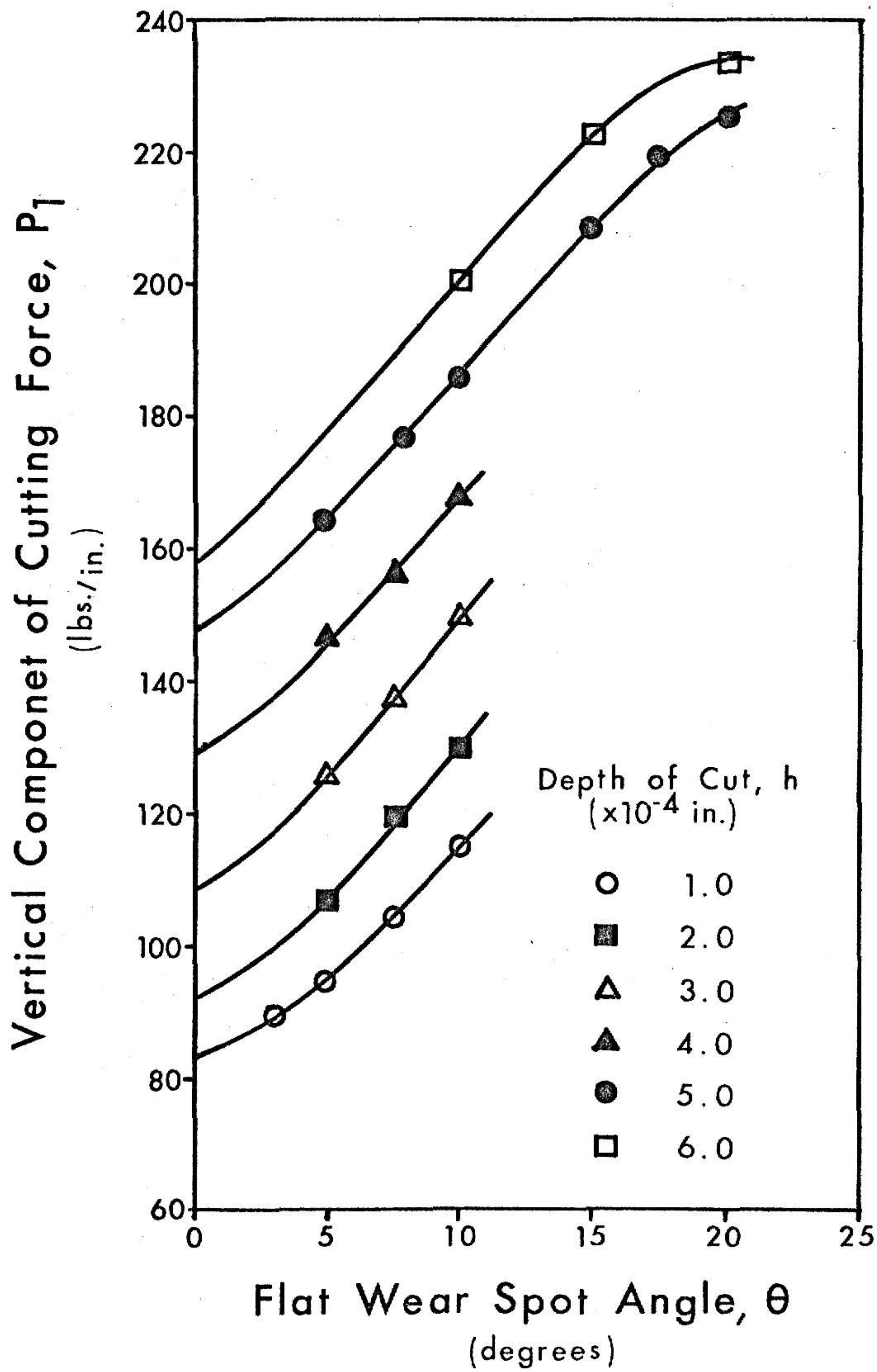

Vertical Component Of Cutting Force, P_1 versus Wear Spot Angle, θ

Figure 13

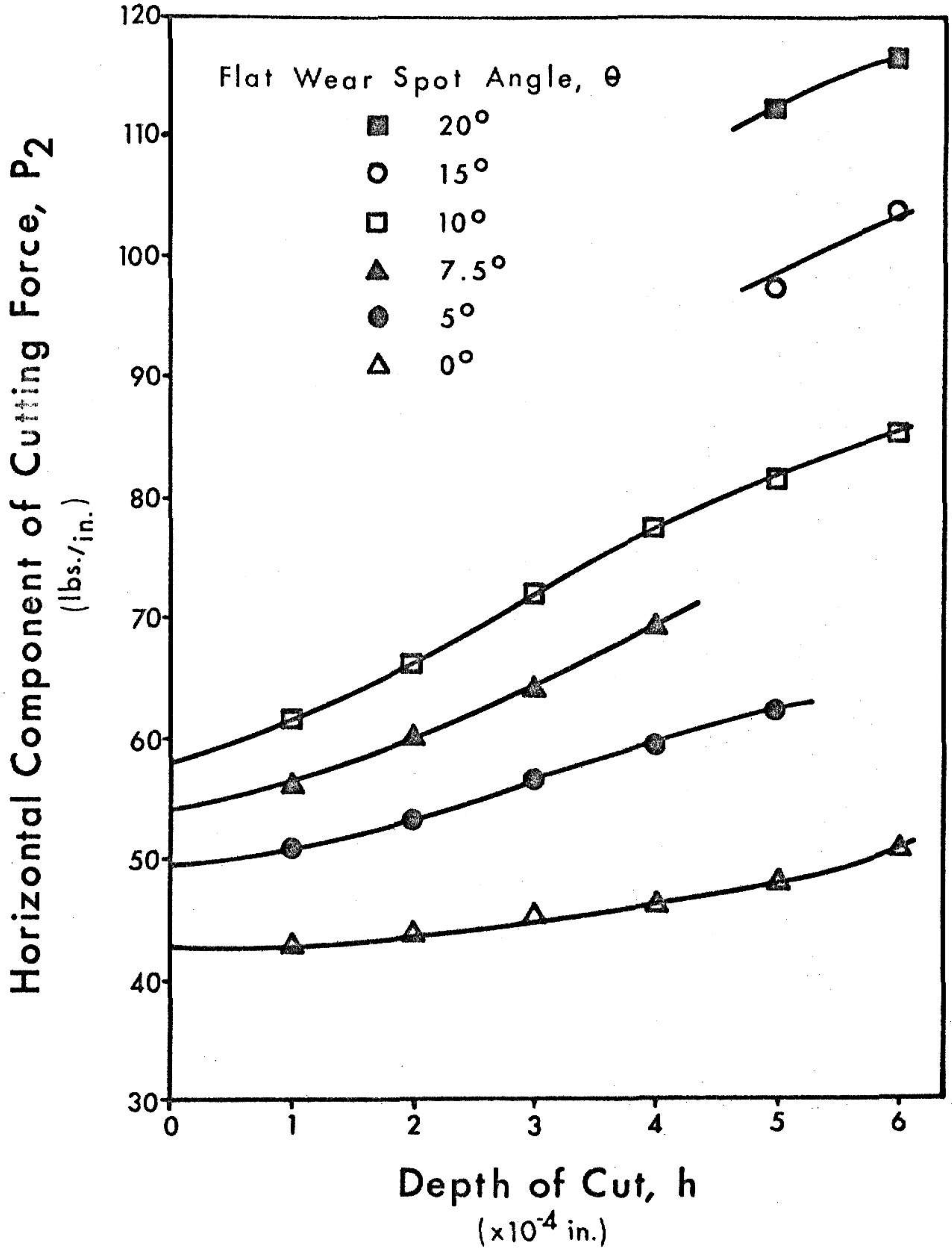

Horizontal Component Of Cutting Force, P_2 versus Depth Of Cut, h

Figure 14

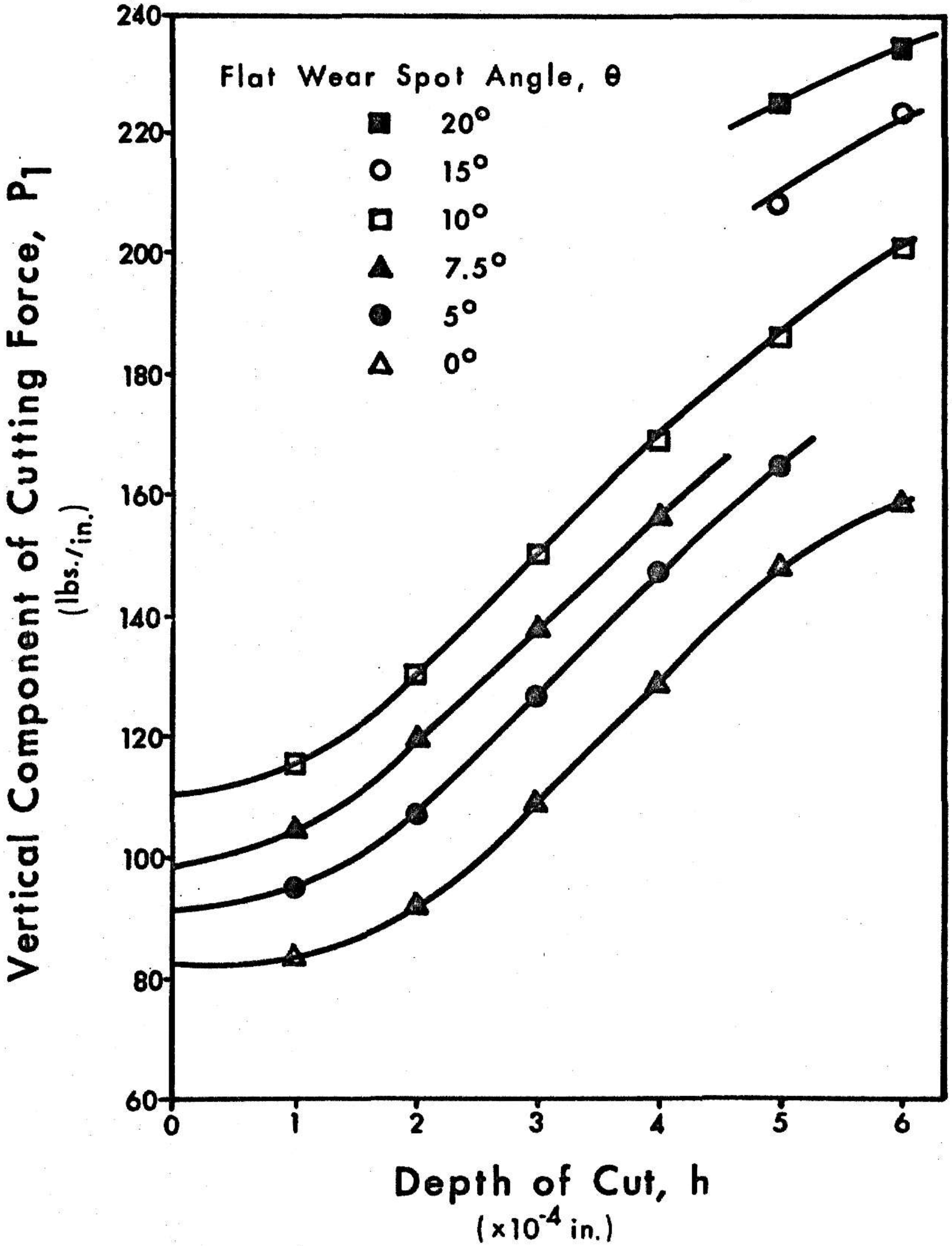

Vertical Component Of Cutting Force, P_1 versus Depth Of Cut, h

Figure 15

Figs. 14 and 15 show the horizontal and vertical cutting forces as a function of the cutting depth, h. A contrast can be seen in that the curves for the vertical forces are much steeper than the curves for the horizontal forces. This means that as larger depths of cut are taken a rapidly increasing force is required to keep the tool at that depth, whereas, there is little increase in the force that does the actual cutting work. The curves in Figs. 14 and 15 also show that there is a "threshold" cutting force which must be reached before any cutting takes place. It is believed by some that the cutting force becomes zero at zero depth of cut and that an increase in force will result in a small depth of cut being taken. As we have shown this is not true, a certain amount of cutting force must exist before any cutting can take place.

The geometry of the cutting action changes with different depths of cut and different flat wear spot angles. This is seen in Figs. 16 and 17 showing the changes caused by the different flat wear spot angles of $\theta = 20°$ and $\theta = 5°$. The stresses on the tool surface also change with different tool geometry as shown in Tables I and II. The normal stress distribution on the tool surface, from Tables I and II, is shown in Fig. 18 and 19 for the case of $\theta = 20$ and $\theta = 5°$, at a depth of cut equal to 0.0005 in.

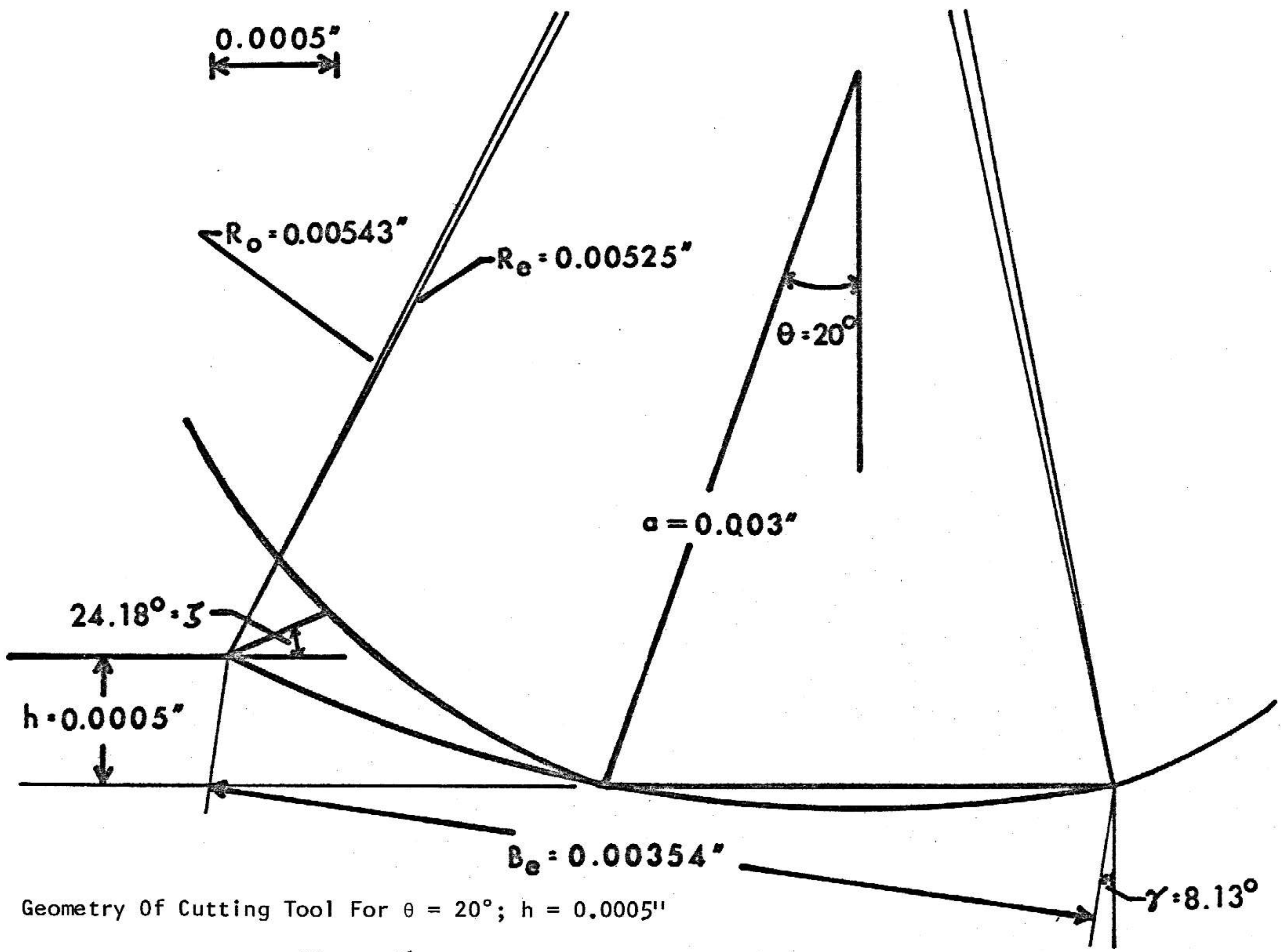

Geometry Of Cutting Tool For $\theta = 20°$; $h = 0.0005''$

Figure 16

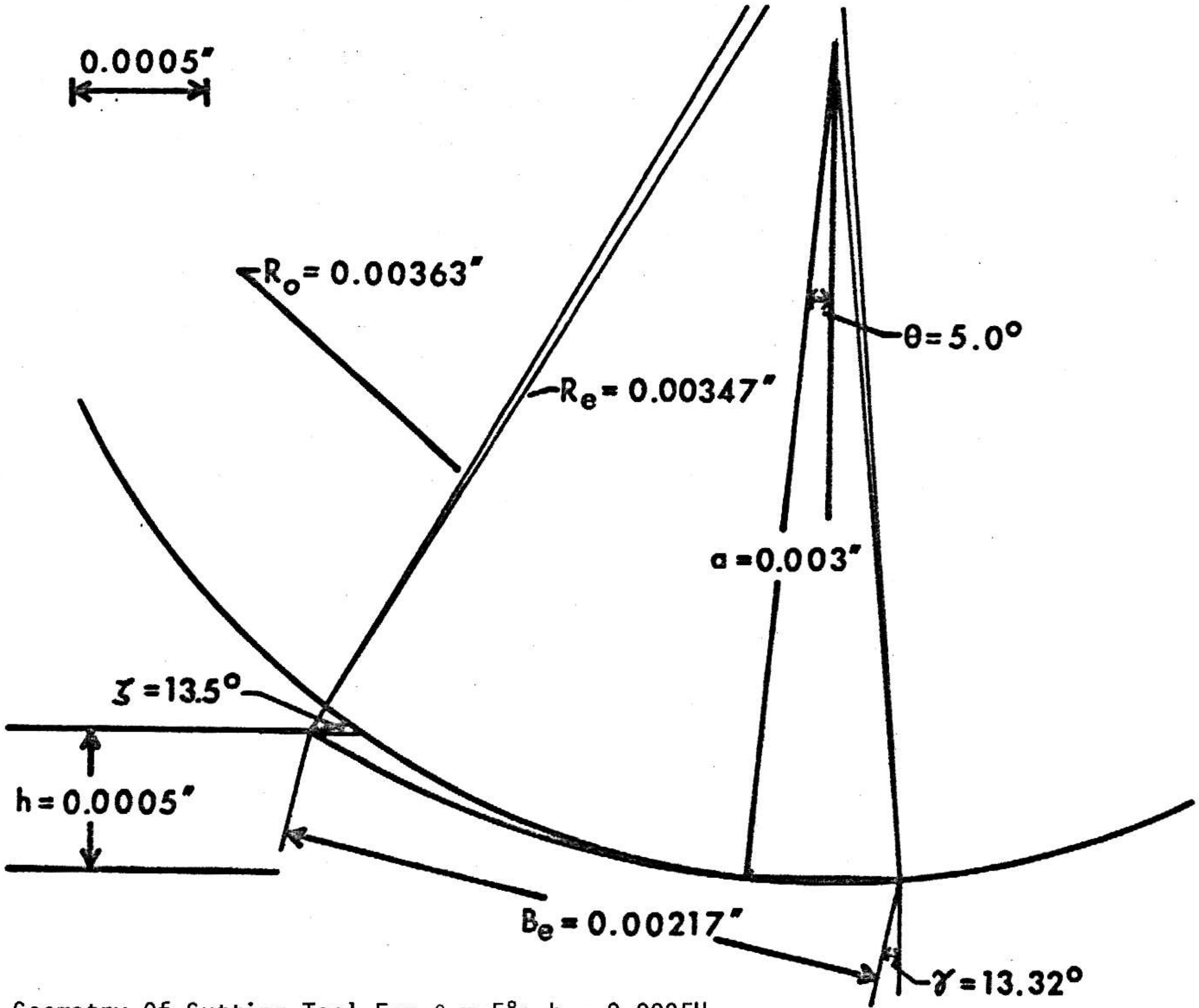

Geometry Of Cutting Tool For θ = 5°; h = 0.0005"

Figure 17

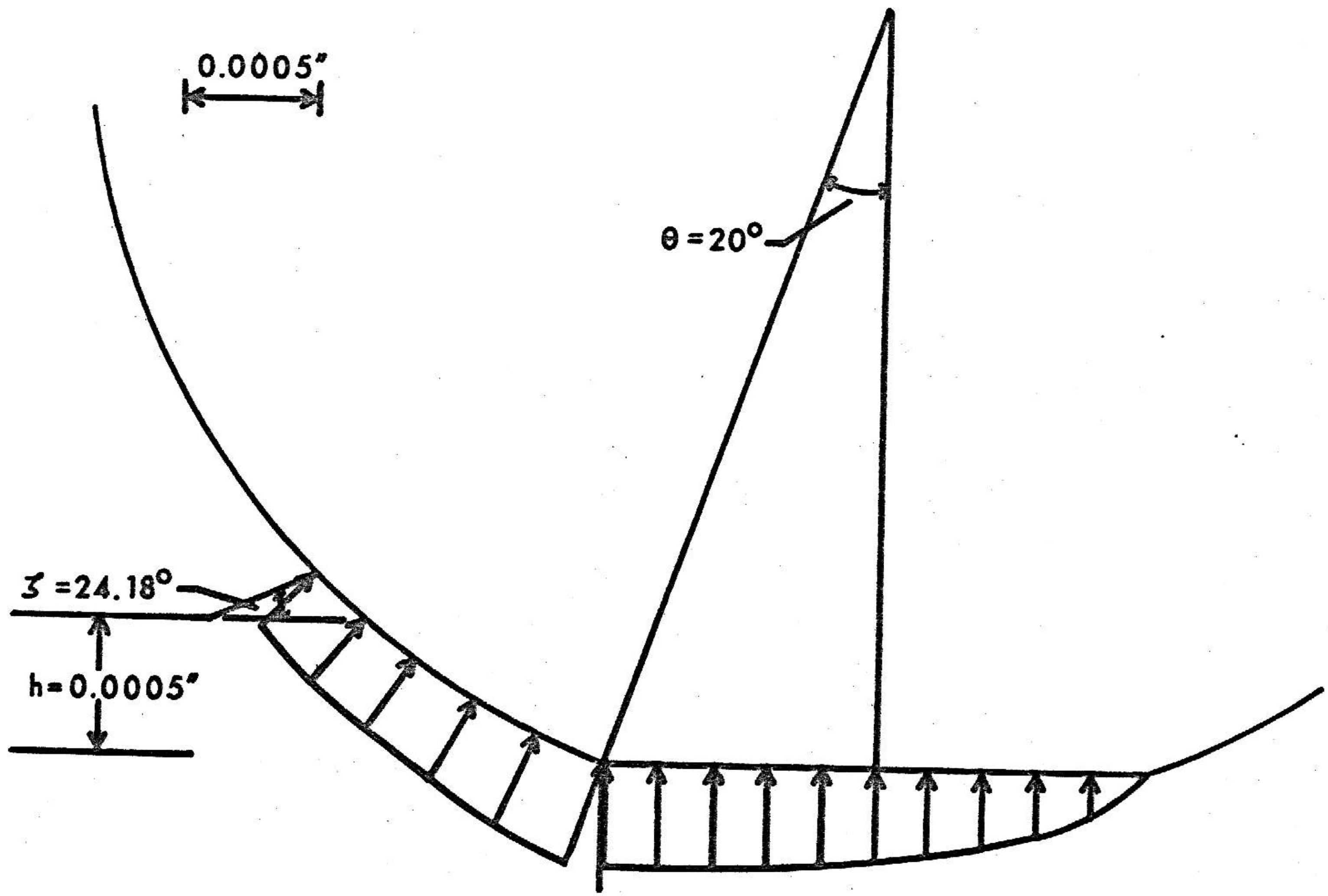

Normal Stress Distribution On Tool Surface For $\theta = 20°$; $h = 0.0005''$

Figure 18

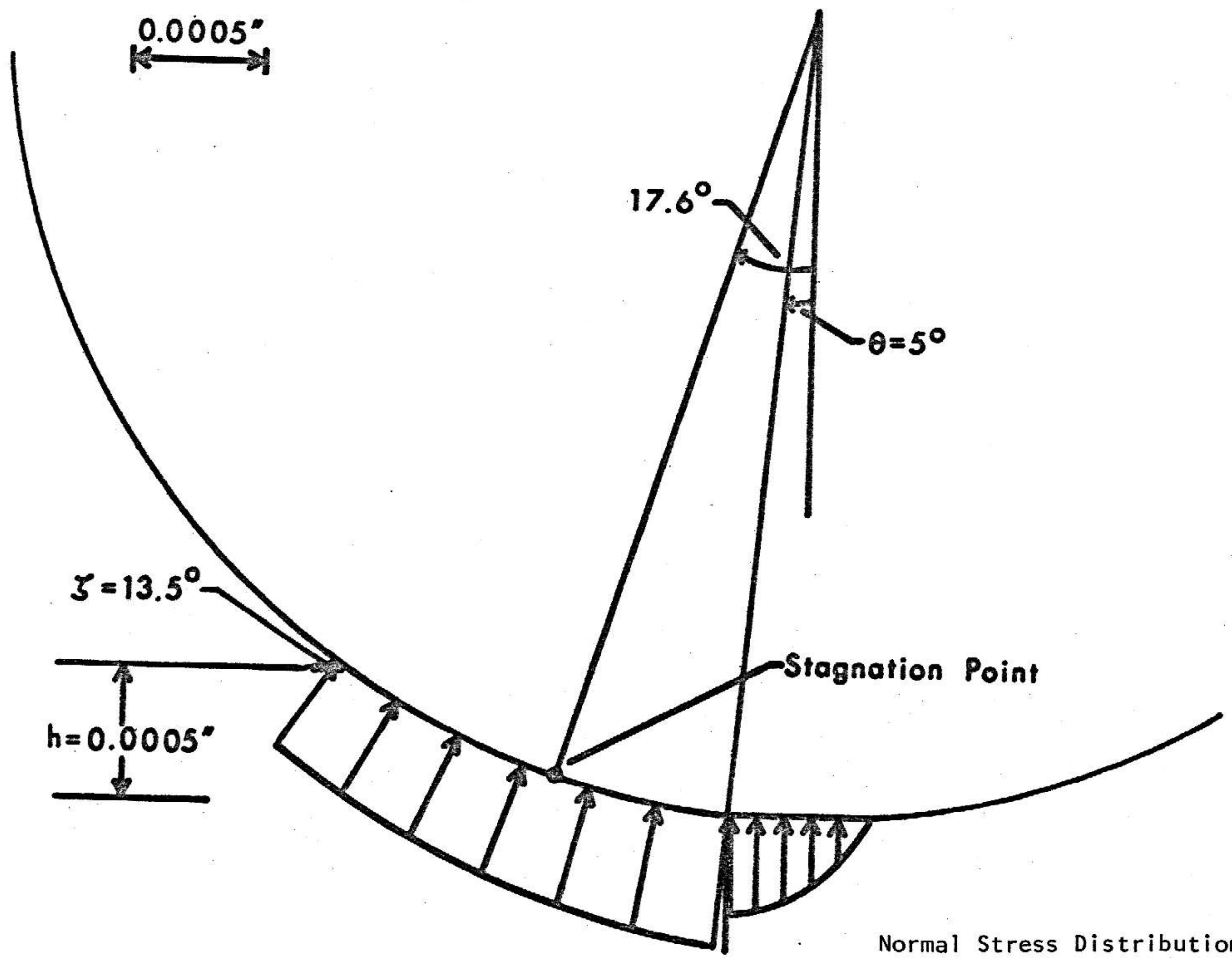

Normal Stress Distribution On Tool Surface
For $\theta = 5°$; $h = 0.0005''$

Figure 19

$\theta = 20°$ $h = 0.0005''$

Λ (deg.)	σ ($\times 10^4$ lbs./in.^{2})	τ ($\times 10^4$ lbs./in.^{2})
-16.29	3.484	2.439
-12.47	4.775	3.343
- 8.55	5.657	3.960
- 4.54	6.302	4.412
- 0.48	6.780	4.746
3.58	7.124	4.987
7.61	7.353	5.147
11.56	7.477	5.234
15.40	7.501	5.251
19.10	7.427	5.199
19.95	9.316	2.871
20.0	7.635	2.670
25.1	7.219	2.608
29.9	6.827	2.545
35.0	6.420	2.474
39.9	6.037	2.401
44.3	5.696	2.331

Stress Distribution on Tool Surface Corresponding to Fig. 18

TABLE I

$\theta = 5°$ $h = 0.0005''$

Λ (deg.)	σ ($\times 10^4$ lbs./in.^{2})	τ ($\times 10^4$ lbs./in.^{2})
- 5.0	0.0	0.0
- 3.71	3.654	2.558
- 1.59	5.038	3.527
0.53	6.007	4.205
2.65	6.742	4.720
4.76	7.314	5.120
4.93	10.245	2.955
5.0	9.807	2.918
10.1	9.367	2.876
14.9	8.955	2.834
20.0	8.524	2.785
25.1	8.097	2.732
29.9	7.700	2.679
35.0	7.282	2.618

Stress Distribution on Tool Surface Corresponding to Fig. 19

TABLE II

CHAPTER VIII

DISCUSSION AND CONCLUSION

The results presented in this thesis show that the horizontal cutting force is about 46 pounds per inch of workpiece width at a cutting depth of 0.0005 in. The experimental work of Abdelmonein and Scrutton showed that the horizontal cutting force for a depth of 0.0005 in. was approximately 50 pounds per 0.25 in. of workpiece width or approximately 200 pounds per inch of width. Although there has been little research done in the area of small depths of cut with negative rake tools, it must be assumed at this time, that these experimental results are represenative of the correct cutting forces.

Since the analysis does not agree with the experimental data it must be assumed that the analysis needs further refinement. One particular region which needs further consideration is that of the location of point D. The assumed location of point D maybe reasonable when considering large flat spots, since any additional area of sliding (which has not been accounted for) is probably small in comparison to the sliding contact on the flat wear spot. But as the angle θ, is reduced, the location of point D becomes more critical since the area of sliding contact on the flat spot is reduced and the area unaccounted for is probably much larger. This means that the location of point D should be further up the trailing edge of the tool. The theory would then include a larger region of the tool contact and a larger cutting force would result.

There is also some doubt about the value of the yield stress in shear which should be used in the analysis. It was assumed that the shear yield stress, K, was constant throughout the material. It was further assumed that the value of K should correspond to the stress relieved state of the material. But the yield stress in the neighborhood of the tool is probably higher due to the strain hardening that takes place in front of the tool. By increasing the value of K, the cutting force required to remove the metal should also increase.

The assumed value of the coefficient of friction acting on the tool, $\mu_2 = 0.7$, might also be too low. Experimental results have shown that the coefficient of friction can vary over a large range and depends largely on the stress levels and the contact surfaces. Due to the fact that the material is highly stressed and the fact that the material sliding surface is a freshly cut clean surface the value of μ_2 may really be much larger than 0.7.

The relocation of point D would lead to substantial changes in the analytical procedure, so this change was not made at this time. But the values of the shear yield stress, K, and the coefficient of friction, μ_2, were easily adjusted to see if better agreement with the experimental results was obtained. Numerical results were obtained for the cases, $\theta = 20°$, h = 0.0005 in. and h = 0.0006 in. The value of the tensile yield stress, S_y, was changed to 70,800 psi from the previous 58,000 psi. The value of μ_2 was also increased to 1.0 from the previous value of 0.7. The analysis for h = 0.0005 in. showed an increase of approximately 40 percent to a horizontal cutting force of 142 pounds per inch. Similarly the horizontal cutting force at a depth of h = 0.0006 in. showed an increase of about 44 percent to a level of 153 pounds per inch.

These horizontal forces are still not quite as large as those found by Abdelmonein and Scrutton but the agreement is much better and it appears that good agreement can be achieved by minor changes of some of the basic assumptions used in the theory.

It is encouraging that the present theoretical results compare as well as they do with experimental values in view of the complex nature of the cutting problem.

CHAPTER IX

RECOMMENDATIONS

To enhance the value of this work, additional work is needed in finding the previously defined point D. The assumption used in this thesis may be reasonable when considering large flat wear spots, but as the wear spot decreases the correct location of this point becomes more critical.

Also deserving further consideration is the location of point C. The previously assumed conditions for finding point C, may not be satisfactory and a better method of finding point C and the radius R_o should inprove the problem analysis.

Further consideration of experimental data is needed to be sure that the right values of material tensile yield stress, S_y, and coefficient of friction, μ_2 are used.

More experimental cutting data is needed to compare with the theoretical results as well as to verify the experimental data of Abdelmoneim and Scrutton. The additional data is needed to add confidence to either the data of Abdelmoneim and Scrutton or the theoretical results.

REFERENCES

1. Ramalingam, S., and J. Hazra. "Dynamic Shear Stress-Analysis of Single Crystal Machining Studies," Journal of Engineering for Industry. (November 1973), pp. 939-944.

2. Timoshenko, S., and J. N. Goodier. Theory of Elasticity, 2nd ed. New York: McGraw-Hill Book Company, Inc., 1951.

3. Poritsky, H. "Stresses and Deflections of Cylindrical Bodies in Contact With Application to Contact of Gears and of Locomotive Wheels," Journal of Applied Mechanics. Trans. ASME, vol. 72, 1950, pp. 191-201.

4. Smith, J. O., and Chang Keng Liu. "Stresses Due to Tangential and Normal Loads on an Elastic Solid with Application to Some Contact Stress Problems," Journal of Applied Mechanics. (June 1953), pp. 157-166.

5. Hamilton, G. M., and L. E. Goodman. "The Stress Field Created by a Circular Sliding Contact," Journal of Applied Mechanics. (June 1966), pp. 371-376.

6. Dumas, G., and C. N. Baronet. "Elastoplastic Indentation of a Half-Space by an Infinitely Long Rigid Circular Cylinder," International Journal of Mechanical Science. Pergamon Press, 1971, vol. 13, pp. 519-530. Printed in Great Britian.

7. Schneider, W. C., and J. B. Cheatham, Jr. "Indentation Analysis for General Shapes of Surface Boundaries and Punch Profiles," Society of Petroleum Engineers Journal. (September 1971), pp. 321-329.

8. Rubenstein, C., F. K. Groszman, and F. Koenigsberger. "Force Measurements During Cutting Tests with Single Point Tools Simulating the Action of a Single Abrasive Grit," Science and Technology of Industrial Diamonds. Vol. 1, pp. 161-172.

9. Abdelmoneim, M. Es., and R. F. Scrutton. "Tool Edge Roundness and Stable Build-Up Formation in Finish Machining," Journal of Engineering for Industry. Transactions of ASME, (November 1974), pp. 1258-1267.

APPENDIX A

COMPUTER PROGRAM

COMPUTER PROGRAM NOMENCLATURE

A	a
H	h
P1P	P_1'
P2P	P_2'
BE	b_e
PO	P_o
EW	E
GAMD	γ
MU	μ
MU2	μ_2
ETAD	η
SY	S_y
RE	R_e
RO	R_o
THETED	θ_e
LAMD	λ
ZETAD	ζ
CHI	χ
OMEGA	Ω
PSI	ψ
TAU	τ

K	K
P1	P_1
P2	P_2
NUW	ν
XI	$\eta(\mu)$
THETAD	θ
FYY	Vertical Force on Tool Nose
FXX	Horizontal Force on Tool Nose
TS1	Vertical Force on Elastic Part of Flat Spot
TTAUAF	Horizontal Force on Elastic Part of Flat Spot
FYF	Vertical Force on Plastic Part of Flat Spot
FXF	Horizontal Force on Plastic Part of Flat Spot
XO	Length of Flat Wear Spot
TFY	Total Vertical Component of Cutting Force
TFX	Total Horizontal Component of Cutting Force

BRIEF DESCRIPTION OF PROGRAM

It is not possible to solve the problem for all cutting conditions using the computer program. Because of this and the non-linear nature of some of the functions, the computer program could not be made fully automatic in finding solutions. Therefore, the computer program was written to match the vertical components of force acting on the equivalent indenter and the vertical component of force acting on the tool by the adjustment of the chip angle, ζ. This was still somewhat of a problem since when θ and h were changed the range of possible values of ζ also changed. This was continually adjusted by limiting the parameters ZI and ZETAD, to the lower and upper limits of this range. Once the vertical components of force were matched, it was necessary to adjust the coefficient of friction acting on the equivalent indenter, MU, and to make the corresponding change in the parameter XI, which is the function $\eta(\mu)$. This step involved the use of trial and error, since the function $\eta(\mu)$ is non-linear. For these reasons the program could be made automatic only by using a numerous amount of checks and subsequent changes in parameters. The trial and error method was therefore used because of the ease of operation. It also enabled us to see what was happening in the program and what must be changed as different problems were tried.

To print the stresses acting on the tool surface and to find the stagnation point it was most expedient to first run the program as many times as necessary to find ζ. Then using this value and activating the desired print statements in the program, the stresses could be printed out.

PROGRAM LISTING

ILLEGIBLE DOCUMENT

THE FOLLOWING DOCUMENT(S) IS OF POOR LEGIBILITY IN THE ORIGINAL

THIS IS THE BEST COPY AVAILABLE

```
$JOB              MLG,TIME=(0,20)
C                        YELLOW BRASS
C       ELASTIC ANALYSIS
        REAL K,MUP,LAMB,LAMBD,MU2,MU3
        REAL NUW,MU,MU1,LAMD,LAMDL,LAMDR,LAM
     21 FORMAT('1',5X,'EW',5X,'NUW',5X,'SY')
     22 FORMAT(/,3X,'MU',5X,'XI')
     23 FORMAT(/,4X,'A',7X,'H',5X,'THETAD')
     24 FORMAT(/,5X,'P1',13X,'P2',11X,'ERR',10X,'P1P',11X,'P2P')
     25 FORMAT(/,4X,'LAMD',11X,'ETAD',12X,'ZETAD',8X,'ASLPO',8X,'THETED')
     26 FORMAT(/,5X,'RO',11X,'CHI',12X,'OMEGA')
     27 FORMAT(/,5X,'RE',12X,'RD',12X,'BE',12X,'PD',11X,'GAMD')
    100 FORMAT(/,5E14.6)
C       MU=0 XI=3.12,MU=.05 XI=3.1,MU=.1 XI=3.06 MU=.15 XI=3.01
C       MU=.2 XI=2.94,MU=.25 XI=2.84,MU=.3 XI=2.63,MU=.35 XI=2.48
C       MU=.4 XI=2.25,MU=.45 XI=2.02,MU=.5 XI=1.78,MU=.55 XI=1.55,
C       MU=.6 XI=1.40
        MU=0.22
        XI=2.92
        ZETAD=10.0
        Z1=10.0
        ASLI=45.0
        THETAD=10.0
        SY=58000.0
        H=0.0005
        MU2=0.7
        Z2=Z1
        RATIO=0.1
        EW=14000000.0
        A=0.003
        PI=3.1415927
        PIC=PI/180.0
        ERROR=0.000001
        NUW=0.3
        THETA=THETAD*PIC
        PRINT 21
        PRINT 50,EW,NUW,SY
     50 FORMAT(/,E10.1,F6.2,F8.0)
        PRINT 22
        PRINT 60,MU,XI
     60 FORMAT(/,F8.4,F8.4)
        PRINT 23
        PRINT 70,A,H,THETAD
     70 FORMAT(/,F8.5,F8.5,F6.2)
        PO=SY*XI/SQRT(3.0)
        SINTHE=SIN(THETA)
        COSTHE=COS(THETA)
        HOA=H/A
        II=0.0
     56 CONTINUE
        ITEST=1
        I=0
     72 CONTINUE
        I=I+2
        IF(I.GT.92) GO TO 181
        GO TO 182
    131 FORMAT(/,3X,'I GT. 92')
    181 PRINT 131
        GO TO 199
    182 LAMD=(I-1)
```

```
      LAM=LAMD*PIC
      IF(COS(LAM).GT.(1.0-HOA)) GO TO 72
   75 CONTINUE
      ITIME=0
      ZETA=ZETAD*PIC
      TANZET=TAN(ZETA)
      TANGAM=COSTHE-COS(LAM)-HOA+TANZET*(SINTHE+SIN(LAM))
      TANGAM=HOA*TANZET/TANGAM
      GAM=ATAN(TANGAM)
      GAMD=GAM/PIC
      ITIME=ITIME+1
      IF(ITIME.GT.80) GO TO 183
      GO TO 184
  132 FORMAT(/,'ITIME GT. 80')
  183 PRINT 132
      GO TO 189
  184 BE=H/SIN(GAM)
      P1P=0.25*PI*BE*PO
C     FINDS RO
      RO1=0.0
      RO2=0.0
      RO=0.05
      NN=0.0
   52 CONTINUE
      NN=NN+1.0
      IF(NN.GT.70) GO TO 165
      GO TO 166
  165 PRINT,RO,NN,AAA,ITIME,I,N,II
  166 CONTINUE
      IF(NN.GT.80) GO TO 185
      GO TO 186
  133 FORMAT(/,3X,'NN GT. 120')
  185 PRINT 133
      GO TO 189
  186 RE=4.0*PO*(1.0-NUW*NUW)/(BE*EW)+1.0/RO
      RE=1.0/RE
      ARG=2.0*RE/BE
      IF(ARG.LT.1) GO TO 151
      GO TO 153
  152 FORMAT(/,7X,'RE',16X,'BE',16X,'RO',16X,'PO',16X,'AAA',14X,'ARG',
     114X,'ZETAD')
  151 PRINT 152
      PRINT,RE,BE,RO,PO,AAA,ARG,ZETAD
  153 CONTINUE
      ARG=1.0/SQRT(ARG*ARG-1.0)
      ANG=ATAN(ARG)
      THETAE=2.0*ANG
      AR=2.0*RO/BE
      THETED=THETAE/PIC
      AR=1.0/SQRT(AR*AR-1.0)
      ETA=ATAN(AR)
      ETAD=ETA/PIC
      CHI=RE*SIN(ANG-GAM)/(A*SINTHE)
      OMEGA=RO*SIN(ETA-GAM)/(A*SINTHE)
      AAA=1.0-CHI+(1.0-OMEGA)/RATIO
      AAA2=ABS(AAA)
      AAA3=0.00002
      IF(AAA2.LT.AAA3) GO TO 64
      IF(AAA) 61,64,63
   61 RO1=RO
```

```
      GO TO 51
   63 R02=R0
      GO TO 51
   51 R0=(R01+R02)/2.0
      GO TO 52
   64 CONTINUE
      ASLP=ANG+GAM+ZETA
      ASLPD=ASLP/PIC
      ERR=(ASLPD-ASL1)/ASL1
      ERR=ERR*ERR
      IF(ERR.LE.EPSUR) GO TO 90
      IF(ITEST.EQ.1.AND.ASLPD.GT.ASL1) GO TO 80
      IF(ITEST.EQ.2) GO TO 82
      ITEST=2
      ASLPDR=ASLPD
      LAMDR=LAMD
      GO TO 82
   80 ASLPDL=ASLPD
      LAMDL=LAMD
      GO TO 72
   82 IF(ASLPD.LT.ASL1) GO TO 84
      ASLPDL=ASLPD
      LAMDL=LAMD
      GO TO 86
   84 ASLPDR=ASLPD
      LAMDR=LAMD
   86 LAMD=(ASL1-ASLPDL)*(LAMDR-LAMDL)/(ASLPDR-ASLPDL)+LAMDL
      LAM=LAMD*PIC
      GO TO 75
   90 P2P=MU*P1P
      P1=P1P*COS(GAM)-P2P*SIN(GAM)
      P2=P1P*SIN(GAM)+P2P*COS(GAM)
C     PLASTIC ANALYSIS
   32 FORMAT(//,5X,'FYY',12X,'FXX')
  201 FORMAT(/,2E14.6)
  302 FORMAT(/,6X,'TSL',10X,'TTAUAF')
  801 FORMAT(/,6X,'MU2',11X,'X0')
  303 FORMAT(/,6X,'TFY',12X,'TFX')
      HH=1.0
      LAM=LAMD*PIC
      THETA=THETAD*PIC
      K=SY/SQRT(3.0)
      R=A
      ZETA=ZETAD*PIC
      ZETAR=ZETA
      PSIB=PI/4.0
      DLAM=(LAM-THETA)/100.0
      LAMB=THETA
      FX=0.0
      FY=0.0
      FYY=0.0
      FXX=0.0
   40 THETAS=0.0
      PHIS=0.0
      PSIA=PI/4.0
      N=0.0
   30 EE=-MU2*(SIN(2.0*PSIA)+2.0*((PI+2.0)/4.0-ZETAR-LAMB+PSIA))
      AA=1.0-COS(2.0*PSIA)-EXP(EE)
      N=N+1.0
      IF(N.GT.80) GO TO 187
```

```
      GO TO 188
  134 FORMAT(/,3X,'N GT. 80')
  187 PRINT134
      GO TO 189
  188 Q=ABS(AA)
      QQ=0.000001
      IF(Q.LT.QQ) GO TO 99
      IF(AA) 10,99,12
   10 THETAS=PSIA
      GO TO 20
   12 PHIS=PSIA
      GO TO 20
   20 PSIA=(THETAS+PHIS)/2.0
      GO TO 30
   99 CONTINUE
      PA=K*SIN(2.0*PSIA)+2.0*K*((PI+2.0)/4.0-ZETAR-LAMB+PSIA)
      TAUA=K*COS(2.0*PSIA)
      AREA=DLAM*R*HH
      FY=PA*AREA*COS(LAMB)+TAUA*AREA*SIN(LAMB)
      FX=PA*AREA*SIN(LAMB)-TAUA*AREA*COS(LAMB)
      LAMBD=LAMB/PIC
      IF(FX.LT.0) GO TO 155
      GO TO 156
  155 FY=PA*AREA*COS(LAMB)-TAUA*AREA*SIN(LAMB)
      FX=PA*AREA*SIN(LAMB)+TAUA*AREA*COS(LAMB)
  156 CONTINUE
      PSIAD=PSIA/PIC
      FYY=FYY+FY
      FXX=FXX+FX
      LAMB=LAMB+DLAM
      IF(LAMB.LT.LAM) GO TO 40
      LAMB=0.0
   45 THETAS=0.0
      PHIS=0.0
      PSIA=PI/4.0
      N=0.0
   46 FE=-MU2*(SIN(2.0*PSIA)+2.0*((PI+2.0)/4.0-ZETAR-LAMB+PSIA))
      AA=1.0-COS(2.0*PSIA)-EXP(FE)
      N=N+1.0
      IF(N.GT.80) GO TO 148
      GO TO 149
  147 FORMAT(/,3X,'N. GT. 80')
  148 PRINT 147
      GO TO 189
  149 Q=ABS(AA)
      QQ=0.000001
      IF(Q.LT.QQ) GO TO 44
      IF(AA) 47,44,48
   47 THETAS=PSIA
      GO TO 49
   48 PHIS=PSIA
      GO TO 49
   49 PSIA=(THETAS+PHIS)/2.0
      GO TO 46
   44 CONTINUE
      PAF=K*SIN(2.0*PSIA)+2.0*K*((PI+2.0)/4.0-ZETAR-LAMB+PSIA)
      TAUF=K*COS(2.0*PSIA)
      AREAF=(1.0-OMEGA)*2.0*R*SIN(THETA)
      FYF=PAF*AREAF
      FXF=TAUF*AREAF
```

```
      XO=2.0*R*SIN(THETA)-((1.0-OMEGA)*2.0*R*SIN(THETA))
      X=0.0
   17 X=X+0.00005
      XP=X/COS(GAM)
      S1P=(2.0*PO/BE)*(SQRT(BE*BE/4.0-(XP-BE/2.0)*(XP-BE/2.0)))
      S1=S1P*(COS(GAM)*COS(GAM)-MU*COS(GAM)*SIN(GAM))
      TAUAF=MU2*S1
      IF(X.LT.XO) GO TO 17
      XOP=XO/COS(GAM)
      TS1=(COS(GAM)*COS(GAM)-MU*COS(GAM)*SIN(GAM))*2.0*PO/BE*
     1(((-2.0*XOP+BE)/(-4.0))*(SQRT(-XOP*XOP+BE*XOP))-(BE*BE/8.0)
     1*(ARSIN((-2.0*XOP+BE)/BE))+BE*BE*PI/16.0)
      TTAUAF=MU2*TS1
      TFY=FYY+FYF+TS1
      T1=P1-TFY
      TFX=FXX+FXF+TTAUAF
      TT1=ABS(T1)
      EE=0.5
  159 FORMAT(/,7X,'T1',13X,'II',10X,'ZETAD')
      PRINT 159
      PRINT,T1,II,ZETAD
      IF(TT1.LT.EE) GO TO 53
      IF(T1) 57,53,54
   54 Z1=ZETAD
      GO TO 55
   57 Z2=ZETAD
      GO TO 55
   55 ZETAD=(Z1+Z2)/2.0
      II=II+1.0
      IF(II.GT.40) GO TO 195
      GO TO 56
  135 FORMAT(/,3X,'II GT. 40')
  195 PRINT 135
      GO TO 189
   53 CONTINUE
  176 FORMAT(/,5X,'WORKPIECE=BRASS')
      PRINT 176
  177 FORMAT(/,5X,'FORCES ARE IN LBS. PER IN. OF WORKPIECE WIDTH')
      PRINT 177
      PRINT 24
      PRINT 100,P1,P2,ERR,P1P,P2P
      PRINT 25
      PRINT 100,LAMD,ETAD,ZETAD,ASLPD,THETED
      PRINT 26
      PRINT 100,RO,CHI,OMEGA
      PRINT 27
  110 PRINT 100,RE,RO,BE,PO,GAMD
  502 FORMAT(/,5X,'P1',13X,'P2',10X,'MU',7X,'RATIO',4X,'ASL1')
      PRINT 502
      PRINT 504
  504 FORMAT(/,12X,'PLASTIC ANALYSIS')
      PRINT 503,P1,P2,MU,RATIO,ASL1
  503 FORMAT(/,E14.6,E14.6,F8.4,F10.4,F10.4)
      PRINT 32
      PRINT 201,FYY,FXX
      PRINT 302
      PRINT 201,TS1,TTAUAF
  501 FORMAT(/,5X,'FYF',12X,'FXF')
      PRINT 501
      PRINT 201,FYF,FXF
```

```
      PRINT 801
      PRINT 201,MU2,XO
      PRINT 303
      PRINT 201,TFY,TFX
C     XO=LENGTH OF FLAT SPOT
  189 CONTINUE
      STOP
      END

$ENTRY
```

APPENDIX B

NUMERICAL RESULTS

θ (deg.)	h (in.)	μ	$\eta(\mu)$	μ	ζ (deg.)	γ (deg.)	b_e (in.)	R_o (in.)	R_e (in.)	P_1 (lbs./in.)	P_2 (lbs./in.)	S.P. (deg.)
3.0	0.0001	0.45	2.07	0.7	37.0	3.37	0.00170	0.0119	0.0106	90.0	46.5	20.75
5.0	0.0001	0.47	2.02	0.7	37.0	3.13	0.00183	0.0121	0.0108	94.5	50.5	
7.5	0.0001	0.475	1.95	0.7	37.5	2.72	0.00211	0.0141	0.0127	105.3	56.2	
10.0	0.0001	0.48	1.90	0.7	37.75	2.43	0.00235	0.0156	0.0141	115.1	61.4	
5.0	0.0002	0.36	2.46	0.7	28.44	6.59	0.00174	0.00536	0.00503	107.3	53.2	
7.5	0.0002	0.39	2.30	0.7	29.88	5.57	0.00206	0.00664	0.00623	110.2	60.1	
10.0	0.0002	0.40	2.25	0.7	30.38	4.99	0.00230	0.00730	0.00687	130.7	66.3	
5.0	0.0003	0.26	2.82	0.7	21.37	9.56	0.00181	0.00392	0.00372	126.5	56.4	
7.5	0.0003	0.30	2.65	0.7	22.88	8.28	0.00208	0.00457	0.00435	137.4	64.2	
10.0	0.0003	0.33	2.57	0.7	23.75	7.38	0.00233	0.00511	0.00487	149.8	72.2	19.06
5.0	0.0004	0.18	2.99	0.7	16.87	11.65	0.00198	0.00366	0.00349	146.9	59.0	
7.5	0.0004	0.24	2.87	0.7	17.75	10.45	0.00220	0.00399	0.00382	156.6	69.1	
10.0	0.0004	0.27	2.80	0.7	18.56	9.43	0.00244	0.00436	0.00418	169.2	77.5	

θ (deg.)	h (in.)	μ	$n(\mu)$	μ_2	ζ (deg.)	γ (deg.)	b_e (in.)	R_o (in.)	R_e (in.)	P_1 (lbs./in.)	P_2 (lbs./in.)	S.P. (deg.)
5.0	0.0005	0.13	3.05	0.7	13.50	13.32	0.00217	0.00363	0.00347	164.3	62.2	17.60
8.0	0.0005	0.19	2.98	0.7	14.06	11.99	0.00241	0.00386	0.00371	177.0	74.3	
10.0	0.0005	0.22	2.92	0.7	14.58	11.17	0.00258	0.00407	0.00392	186.1	81.4	
15.0	0.0005	0.28	2.73	0.7	16.50	9.32	0.00309	0.00488	0.00470	208.6	97.2	
17.5	0.0005	0.30	2.65	0.7	17.25	8.62	0.00334	0.00528	0.00509	219.6	104.0	
20.0	0.0005	0.33	2.57	0.7	24.18	8.13	0.00354	0.00543	0.00525	225.3	112.0	
10.0	0.0006	0.18	2.99	0.7	11.25	12.70	0.00273	0.00395	0.00380	201.0	85.2	
15.0	0.0006	0.25	2.84	0.7	12.81	10.80	0.00320	0.00455	0.00439	223.5	103.2	
20.0	0.0006	0.30	2.68	0.7	27.0	9.74	0.00355	0.00463	0.00449	233.4	116.5	
20.0	0.0005	0.33	2.61	0.7	26.25	8.25	0.00348	0.00518	0.00498	274.9	137.5	
20.0	0.0005	0.50	1.78	1.0	32.5	7.21	0.00398	0.00785	0.00757	211.7	141.8	
20.0	0.0006	0.475	1.96	1.0	32.0	8.87	0.00389	0.00614	0.00595	224.0	152.4	

ACKNOWLEDGEMENTS

I would like to thank Dr. F. C. Appl for his assistance and advice. I am also grateful for financial support given by Kansas State University and Christensen Diamond Products Company. I would very much like to thank my wife, Denise, for her help with the drawings and the typing as well as for her patience and understanding love during the time I was in school.

VITA

MICHAEL LYNN GOYEN

Candidate for the Degree

Master of Science

THESIS: Theory of Cutting with Large Negative Rake Cutting Tools

MAJOR FIELD: Mechanical Engineering

BIOGRAPHICAL:

Personal Data: Born February 21, 1953 at Pratt, Kansas; the son of Lester D. and Delores D. Goyen.

Education: Graduated from high school at Pratt, Kansas in 1971; received an A.S. degree from Pratt Community Junior College in 1973; received a B.S. in Mechanical Engineering from Kansas State University in 1975; completed requirements for the M.S. degree in October 1976.

THEORY OF CUTTING WITH LARGE NEGATIVE RAKE CUTTING TOOLS

by

MICHAEL LYNN GOYEN

B.S., Kansas State University, 1975

AN ABSTRACT OF A MASTER'S THESIS

Submitted in Partial Fulfillment of the

Requirements for the Degree

MASTER OF SCIENCE

Department of Mechanical Engineering

Kansas State University

Manhattan, Kansas

1976

ABSTRACT

Since cutting technology is such an essential part of the materials processing needed for the industrialized society of today, there is a substantial need for research on this subject.

The purpose of this work, was to analyze the cutting process of large negative rake tools at small depths of cut. To do this the approach of an equivalent indenter was used along with plastic slip-line theory. The use of these two approaches aids in the description of the cutting process of large negative rake tools.

The numerical results differ somewhat from the experimental data, but the solution should become better as more refinements are made. It is encouraging that the present theoretical results compare as well as they do with experimental values in view of the complex nature of the cutting problem.